PROBING THE INTERACTION BETWEEN DAPTOMYCIN AND MODEL MEMBRANES

by

Jin Zhang

B.Sc., Nanjing University, 2012

A THESIS SUBMITTED IN PARTIAL FULFILLMENT OF

THE REQUIREMENTS FOR THE DEGREE OF

MASTER OF SCIENCE

in

THE FACULTY OF GRADUATE AND POSTDOCTORAL STUDIES

(Chemistry)

THE UNIVERSITY OF BRITISH COLUMBIA

(Vancouver)

August 2015

Abstract

Daptomycin is the first approved antibiotic from the lipopeptide family, with antibacterial activity against a wide variety of Gram-positive bacteria. It is composed of 13 amino acids with a fatty acyl chain attached at the N-terminus. Although it has been approved for clinical usage for over two decades and a number of studies have worked on the mechanism, many details of the mode of action of daptomycin still remain to be understood. This thesis focuses on shedding light on: i) how daptomycin binds to membranes and whether it forms well-defined oligomers; and ii) whether once in the membrane, daptomycin causes leakage. We have used photon correlation spectroscopy (PSC) to determine the condition under which fusion among vesicles occurs in the presence of daptomycin. 1-palmitoyl-2-oleoyl-*sn*-glycero-3-phosphocholine/1-palmitoyl-2-oleoyl-*sn*-glycero-3-phospho-(1'-*rac*-glycerol) (POPC/POPG) liposome is a better system as higher concentrations of Ca^{2+} is required to trigger membrane fusion. Based on these findings of membrane fusion caused by daptomycin, binding and kinetics experiments were conducted to study the interaction between daptomycin and the lipid membrane. The binding between daptomycin or NBD-labeled daptomycin and POPC/POPG or 1,2-dimyristoyl-d54-*sn*-glycero-3-phosphocholine/1,2-dimyristoyl-*sn*-glycero-3-phospho-(1'-rac-glycerol) (DMPC/DMPG) liposomes is strong, with micromolar dissociation constants. Förster resonance energy transfer (FRET) experiments were conducted under conditions where fusion is not present. The results show that the oligomerization number n is concentration-dependent. A two-stage equilibrium process is proposed when the daptomycin binds and oligomerizes in the membrane, in which daptomycin accumulates firstly in the membrane to form larger oligomers, facilitating further effects which lead to the cell death, such as the lipid

extracting effect on the membrane. In addition, fluorescence experiments were conducted to investigate whether daptomycin causes leakage in POPC/PG and DMPC/PG liposomes, with or without the proton ionophore carbonyl cyanide *m*-chlorophenyl hydrazine (CCCP). Experiments using the ion-selective pore-forming aurein peptide were also done, as a control. For stable liposomes, daptomycin does not cause ion permeabilization of the membrane, suggesting that the membrane depolarization resulting from daptomycin is different from pore-formation by the aurein peptide. The work described in this thesis provides evidence leading to a clearer mechanism of action for daptomycin.

Preface

The work presented in this thesis is the outcome of various collaborations with other scientists. Their contributions are summarized as follows.

Chapter 2 is based in part on a publication (currently under revision): "Jin Zhang, Walter R.P. Scott, Frank Gabel, Miao Wu, Ruqaiba Desmond, JungHwan Bae, Giuseppe Zaccai, W. Russ Algar, and Suzana K. Straus. Concentration effects: Implications on the mechanism of action of daptomycin, BBA Biomembrane, 2015". My supervisor, Dr. Suzana K. Straus, and Dr. W. Russ Algar designed the experiments, helped with the interpretation and discussion of the results. I performed all the fluorescence experiments and analyzed the data. Miao Wu provided guidance for these experiments. Dr. Suzana K. Straus wrote the manuscript. I wrote this chapter and Dr. Suzana K. Straus edited it.

Chapter 3 is based on currently unpublished work. I performed the experiments and data analysis, and wrote this chapter. My supervisor Dr. Suzana K. Straus helped with the design of the experiments, the interpretation and discussion of the results. I wrote this chapter and Dr. Suzana K. Straus edited it.

Table of Contents

List of Tables

List of Figures

List of Abbreviations

POPC	1-palmitoyl-2-oleoyl-*sn*-glycero-3-phosphocholine
POPG	1-palmitoyl-2-oleoyl-*sn*-glycero-3-phospho-(1'-*rac*-glycerol)
DMPC	1,2-dimyristoyl-d54-*sn*-glycero-3-phosphocholine
DMPG	1,2-dimyristoyl-*sn*-glycero-3-phospho-(1'-rac-glycerol)
CL	cardiolipin, 1',3'-bis[1,2-dimyristoyl-*sn*-glycero-3-phospho]-*sn*-glycerol
Rh-PE	1,2-dioleoyl-*sn*-glycero-3-phosphoethanolamine-N-(lissamine rhodamine B sulfonyl)
NBD-Cl	4-Chloro-7-nitrobenzofurazan
HEPES	4-(2-hydroxyethyl)piperazine-1-ethanesulfonic acid
EDTA	Ethylenediaminetetraacetic acid
CCCP	Carbonyl cyanide *m*-chlorophenyl hydrazine
GUV	Giant unilamellar vesicle
LUV	Large unilamellar vesicle
LTA	Lipoteichoic acid
FRET	Förster resonance energy transfer

PCS	Photon correlation spectroscopy
NMR	Nuclear magnetic resonance
MIC	Minimum inhibitory concentration
AMP	Antimicrobial peptide
S. aureus	*Staphylococcus aureus*
E. faecalis	*Enterococcus faecalis*
E. hirae	*Enterococcus hirae*
B. megaterium	*Bacillus megaterium*
B. subtilis	*Bacillus subtilis*
B. anthracis	*Bacillus anthracis*
S. roseosporus	*Streptomyces roseosporus*
A. utahensis	*Antinoplanes utahensis*
S. pyogenes	*Streptococcus pyogenes*
S. lividans	*Streptomyces lividans*
MRSA	Methicillin-resistant *Staphylococcus aureus*

Acknowledgements

I would like to offer my enduring gratitude to my supervisor Dr. Suzana K. Straus for her support and help to my study and research, for her patience, guidance and inspiration over the past three years. Her exceptional expertise in chemistry, her passion to do innovative research, and her kindness and wisdom have motivated me a lot through my graduate study. I feel that I am extremely fortunate to be in her group.

I would like to express my gratitude to Dr. W. Russ Algar for his help and guidance for the experiments. I would also like to thank all of the group members for their help: Dr. Walter R.P. Scott, Yurou Sang, Prashant Kumar, Rui Zhang, Chantal Mustoe, Joseph Lee, Selina Suleman, Michael Nguyen and Ruqaiba Desmond. We have together built a great environment for research and lifelong friendship. I would also like to acknowledge the faculty and staff at UBC for their help.

Special thanks to my thesis committee members, Dr. W. Russ Algar, Dr. Hongbin Li and Dr. Don Fleming, for their invaluable suggestions and comments on my thesis.

Finally, special thanks are owed to my parents and my husband for their unreserved support. They always offer unconditional support and love. With them by my side, my failures hurt less and my successes are greater.

Chapter 1: Introduction

Infectious diseases are one of the leading causes of morbidity and mortality worldwide, especially in developing countries. Approximately 15% of global deaths come from infectious diseases in 2013, based on the latest Global Burden of Disease Study [1]. Antimicrobial agents have been used clinically for the past 70 years for the treatment of infectious diseases [2]. Although these effective agents have dramatically decreased the number of illnesses and deaths from infectious diseases since the 1940s, bacterial strains become resistant to them after long-term and widespread use for human and livestock, reducing the effectiveness of conventional antimicrobial drugs. The growth of antimicrobial resistance to conventional antibiotics has a high rate of increase [3]. The Infectious Disease Society of America predicted that over 70% of the pathogenic bacteria which are responsible for potentially fatal infections in 2004 would develop resistance to at least one of the potent antibiotics designed for treatment. Additionally, since most of the new antibiotics are generally slightly modified versions of the parent antibiotic, resistant strains become resistant to the new antibiotics quickly. According to the estimation of the Centers for Disease Control and Prevention, more than two million people in the United States get infected each year with antibiotic-resistant bacteria, and at least 23,000 deaths are directly caused by these antibiotic-resistant infections [4]. As the growing antibiotic resistance has become a worldwide public health issue, it is imperative to develop novel classes of antibacterial compounds to combat antimicrobial-resistant pathogens. Among the potential alternatives, ubiquitous antimicrobial peptides (AMPs) and potent lipopeptides, represent promising therapeutic options for infections caused by antibiotic-resistant bacteria [5].

1.1 Antimicrobial peptides

AMPs are an essential component of the innate immune system, which is a principal part in the defense system for most known lifeforms, including bacteria, fungi, plants, and animals [6]. They have remained effective throughout evolution for the survival of the host as they can act through a nonspecific mechanism, through direct antimicrobial activity and/or immunomodulatory activity [7]. Table 1.1 is a listing of some peptides with antimicrobial activity and/or immunomodulatory activity in development or clinical trials. AMPs defend the host after microbial infection, and act as a supplement to the highly specific acquired immune system. AMPs have stimulated research and clinical interest for the past two decades. Since then, more than 2000 kinds of AMPs have been isolated and identified from a wide variety of organisms, including bacteria, fungi, plants and animals. A few AMPs have officially entered preclinical and clinical phases to treat diabetic foot ulcers, rosacea, chronic bacterial middle-ear infection and nasally colonized Methicillin-resistant *Staphylococcus aureus* (MRSA) [8].

Table 1.1 Selected peptides with antimicrobial activity and/or immunomodulatory activity in commercial development (This table is reproduced from [7].)

Company	Drug	Stage of development	Medical use
AM-Pharma (Bunnik, The Netherlands)	hLF-1-11	Phase II	Allogeneic bone marrow stem cell transplantation-associated infections
BioLineRx Ltd (Jerusalem, Israel)	BL2060	Preclinical	Gram-negative pneumonia
Ceragenix (Denver, Colorado, USA)	CSA-13/CGX313	Preclinical	Prevention of nasal carriage of *Staphylococcus*
Helix Biomedix (Bothell, Washington, USA)	Lipohexapeptide	Preclinical	Anti-infective
Inimex (Burnaby, British Columbia, Canada)	IMX942	Preclinical	Immunomodulation; treatment of fevers and neutropenia in chemotherapy patients
Migenix Inc. (Vancouver, British Columbia, Canada)	CPI/MX-226	Phase IIIb	Prevention of catheter-related infections
Migenix Inc. (Vancouver, British Columbia, Canada)	CLS001	Phase II+	Inflammation in Rosacea
Novozymes A/S (Bagsvaerd, Denmark)	Plectasin	Preclinical	Systemic anti-Gram positive, especially pneumococcal infections
Pacgen (Vancouver, British Columbia, Canada)	PAC113	Phase IIb	Oral candidiasis
Polymedix (Radnor, Philedelphia, USA)	PMX30063	Phase I	Systemic anti-infective peptidomimetic

A number of attractive features of AMPs make them a novel antibiotic class with a bright future. AMPs have a broad antimicrobial spectrum against microorganisms. They are not only capable of killing bacteria and fungi, but also can be used to treat parasitic infections, and may even be effective for the treatment of cancer and HIV infection [9-11]. Moreover, since AMPs generally kill bacteria through a mechanism targeting the membrane, it is not easy for the strains to acquire resistance to the AMPs. In addition, AMPs are a natural part of the immune system, leading to a lower possibility of having adverse side effects compared to conventional chemical antibiotics.

1.1.1 Structures

Since the sources of the AMPs are diverse, AMPs have various lengths, sequences and structures. AMPs are relatively small, usually with a length of 6 to 100 amino acids. Regardless of the structural diversity, there are two common features shared among the identified AMPs. The majority of AMPs have a net positive charge (generally +2 to +9), due to the presence of basic residues, such as arginine, lysine and histidine. When interacting with or inserting into membranes, AMPs fold and rearrange into amphipathic conformations, with hydrophobic and positively charged parts facing in opposite directions, making it favorable for AMPs to bind efficiently to bacterial cell membranes, which contain lipids with negatively charged headgroups. Structural statistics from the Antimicrobial Peptide Database show that only 13% of identified AMPs have a known 3D structure (β-sheets, α-helices, loop and extended structures [12], as presented in Figure 1.1), determined by solution NMR spectroscopy and X-ray diffraction, while the 3D structures of most identified AMPs have not yet been solved.

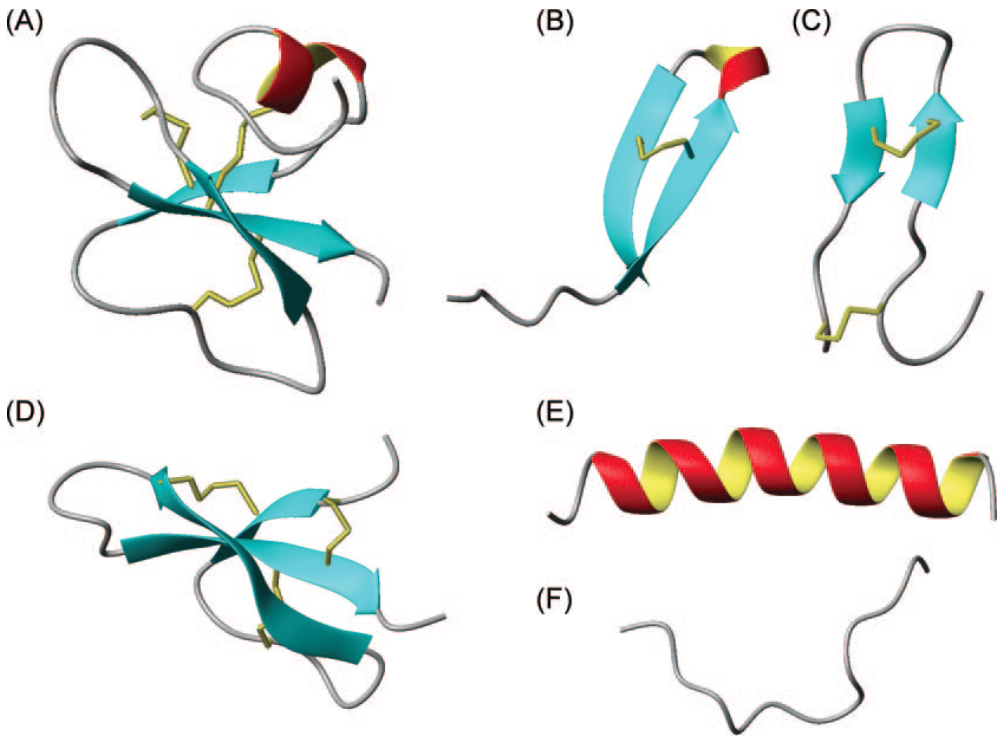

Figure 1.1 Structural classes of antimicrobial peptides, adapted from [6]. (A) Mixed structure of human β-defensin-2 [13]; (B) β-sheeted thanatin with one disulfide bond [14]; (C) β-sheeted polyphemusin with two disulfide bonds[15]; (D) rabbit kidney defensin-1[16]; (E) α-helical magainin-2 [17]; (F) extended indolicidin [18].

1.1.2 Mechanism

Extensive studies have been conducted in order to understand the mode of action of AMPs. Most of the experimental work has been done on the interaction of AMPs with model membrane systems. A few studies have also been carried out on whole bacterial cells using membrane potential sensitive dyes and fluorescently labeled peptides [19]. Although there is no general agreement among scientists with respect to the concrete mechanism of action of AMPs, there are two main proposed mechanisms of action of AMPs with membranes on the basis of these studies: i) membrane disruptive model which includes the carpet, barrel stave, toroidal pore models and

micellar aggregate models; ii) non-membrane disruptive model targeting intracellular compounds (Figure 1.2) [6].

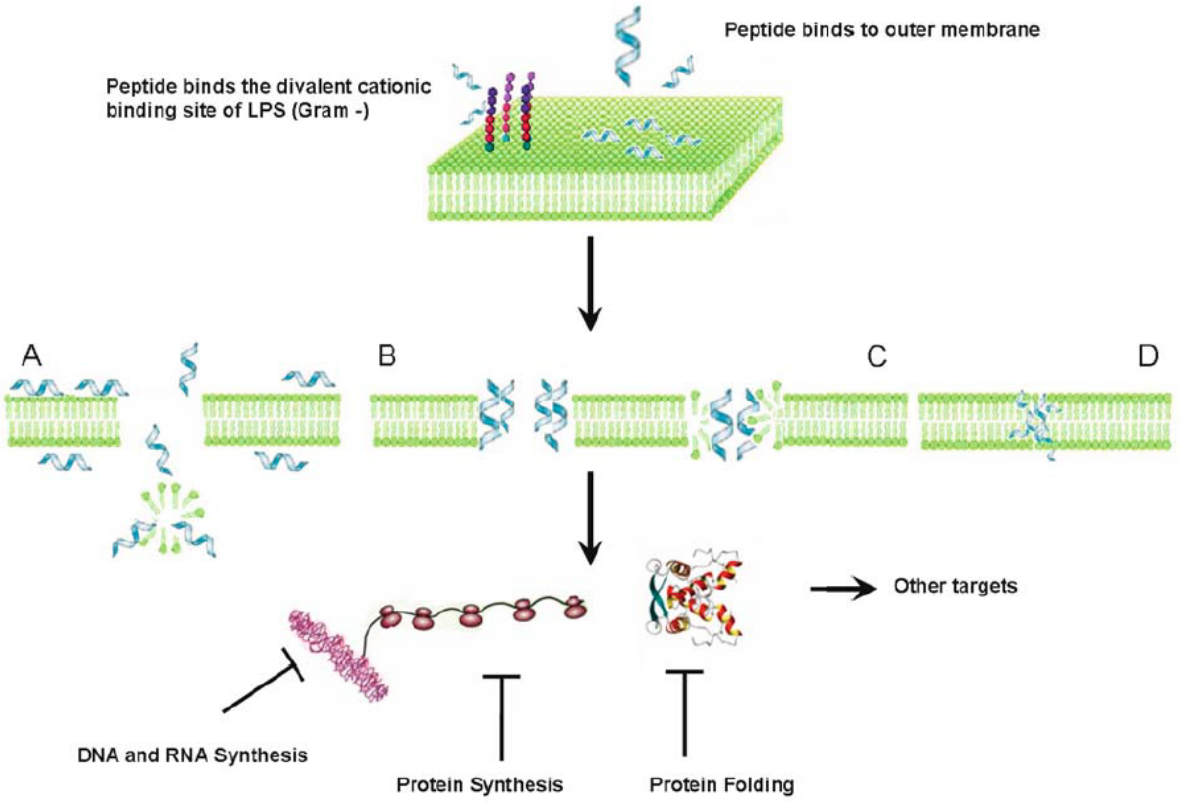

Figure 1.2 Mode of action of AMPs. The listed models explaining the mechanisms of membrane permeabilization include: carpet model (A), barrel stave model (B), toroidal pore model (C), and aggregate model (D). This figure is adapted from [20].

The AMPs, most of which are cationic, initially interact with the bacterial membrane through electrostatic interactions between the peptide and anionic phospholipids, which are present in bacterial cell membranes, but not in mammalian cell membranes. In the membrane-disruptive model, the binding of the AMPs leads to the destabilization of bacterial membranes through a membrane thinning effect [21] followed by a disruptive effect on the membrane or the

translocation of AMPs into the cytoplasm, causing fatal effects on the normal function of the cell. In the non-disruptive mechanism, the AMP molecules pass through and dissociate from the membrane, binding to intracellular polyanions such as DNA and RNA or inhibiting other intracellular molecules [22].

A few AMPs may display their antimicrobial activity in a moderately diffuse way, which is called the carpet mechanism. The initial interaction between the peptide and the membrane is through electrostatic interactions, with peptides carpeting the surface of the outer layer of the membrane. When the peptide density binding to the membrane is over a certain threshold, an excessive amount of curvature strain on the membrane leads to disruption of the membrane. In this mechanism, it is not necessary for the peptides to insert into the membrane core or to form pores or channels in the membrane.

Another model termed the barrel stave mechanism is proposed for some peptides. The peptides initially bind to the membrane surface as monomers, then the hydrophobic part of the peptide inserts perpendicularly into the membrane after a conformational transition. After a concentration threshold of bound peptide is reached, peptide monomers oligomerize, transfer into a transmembrane conformation, and insert deeper into the hydrophobic membrane, since aggregation minimizes the exposure of the hydrophilic portion of peptides to the hydrophobic membrane core. For α-helical peptides, a minimum length of 22 amino acid residues is required to transverse the lipid bilayer, while the minimum length for a β-sheet is around 8 amino acids [23]. The resulting transmembrane pore or channel leads to an efflux of ions, thus killing bacteria.

A model which is between the carpet and barrel-stave mechanisms is the toroidal pore model. It was first proposed by Matsuzaki et al. [24] to explain the mode of action of magainin 2. This model is an extension of the barrel stave model, with transmembrane pores formed by both peptides and lipids. The membrane is subjected to positive curvature strain and curves inward to form the hole. Furthermore, unlike the other two models which require a minimum peptide concentration, the formation of the toroidal pore and translocation of the peptide are dependent on a critical peptide-lipid ratio. When the peptide concentration is over a given limit, the stability of the pore is reduced due to increased electrostatic repulsion between the positively charged portions [25].

All the carpet, barrel stave and toroidal pore mechanisms discussed above suggest that antimicrobial activity against pathogens comes from the disruption of membrane integrity. However, several studies demonstrate that permeabilization is a necessity but may not be sufficient to explain AMP killing activity. In order to explain this observation, the aggregate channel model was proposed [22]. The membrane-bound peptides form aggregates which are not structured, thereby facilitating the formation of pores that span the membrane only for short periods of time. In this model, AMPs would be able to enter the inside of the cell, interfere with synthesis of essential molecules, and lead to cell death due to a lack of crucial cell components.

The non-membrane disruptive mechanism is proposed because some evidence indicates that cell death may occur with relatively little membrane disruption, suggesting that AMPs may interact with several key intracellular targets, including the cell wall, cell division and macromolecular biosynthesis [19, 26]. Therefore, the antibacterial mode of action of AMPs can be more complicated than just membrane disruption, as it also involves some other mechanisms.

1.2 Lipopeptides

Another promising alternative to conventional antibiotics is lipopeptides. Lipopeptide antibiotics are an old class of antibiotics that were discovered over 50 years ago. They include the widely used polymyxin [27] and newer members such as daptomycin [28]. In the past decades, studies on lipopeptides have attracted growing interest due to their activity against multi-resistant bacteria, fungi and viruses. They are also touted as displaying little resistance: commercially available lipopeptides are listed in Table 1.2 [29].

Table 1.2 Selected lipopeptide antibiotics currently in preclinical and clinical stages (Table is reproduced from [29].)

Compound name (commercial name)	Therapeutic area	Method of manufacture	Lead compound and producing organism	Company	Phase
Daptomycin (Cubicin)	Complicated infections of skin and skin structure/ *S. aureus* bacteremia and right-sided endocarditis	Fermentation	Daptomycin and *Streptomyces roseosporus* NRRL11379	Cubist	Market
CB-182, 804	Gram-negative infections	Semi-synthetic	--------	Cubist	IND[1]
WAP-8294A_2	MRSA infections	Fermentation	WAP-8294A_2 and *Lysobacter* sp.	aRigen	Phase I
NAB739 & NAB7061	MDR Gram-negative bacterial infections	Semi-synthetic	Polymyxin B/colistin and *Bacillus polymyxa*	Northern Antibiotics	Preclinical
MX-2401	Serious Gram-positive bacterial infections	Semi-synthetic	Amphomycin and *Streptomyces canus* ATCC 12237	Migenix	Preclinical
Lipohexapeptides HB1275 & HB1345	Acne, rosacea, MRSA and coutaneous mycoses	Synthetic	HB1275 & HB1345 None	Helix Biomedix	Preclinical
Telavancin	Complicated skin and skin structure infections (cSSSI) caused by Gram-positive bacteria	Semi-synthetic	Vancomyncin and *Amycolatopsis orientalis*	Theravance	NDA[2]
Caspofungin (Cancidas)	Antifungal	Semi-synthetic	Echinocandins and *Glarea lozoyensis*	Merck and Co.	Market
Micafungin (Mycamine)	Antifungal	Semi-synthetic	Echinocandins and *Coleophoma empetri*	Astellas Pharmaceuticals	Market
Anidulafungin (Eraxis)	Antifungal	Semi-synthetic	Echinocandins and *Aspergillus nidulans*	Pfizer Pharmaceuticals	Market

[1]: Investigational New Drug Application Process; [2]: New Drug Application Process

Natural lipopeptides are mainly produced nonribosomally in various fungal and bacterial genera during cultivation on various carbon sources [30]. However, lipopeptides, which have been studied most are semi-synthetic in nature, i.e. derivative is obtained from a parent lipopeptide isolated from a microorganism in order to improve the antibacterial activity of this complex.

AMPs and lipopeptides have some features in common, such as their interaction with the membrane and their capacity to fold into amphipathic molecules when interacting with the membrane. More differences, however, exist between them. Contrary to AMPs, which are produced ribosomally and generally have positive charge, lipopeptides are produced through non-ribosomal pathways, with either net positive or negative charge. Moreover, some recent studies indicate that many AMPs isolated from mammals also have immunomodulatory and immunostimulatory activities, meaning that these AMPs somehow work between the innate and adaptive immune systems [29].

1.2.1 Structures

Lipopeptides are generally composed of linear or cyclic peptides, with a lipid tail invariably attached at the N-terminus. The peptide portion is often relatively short with 6 to 7 amino acid residues [31], with an overall negative or positive charge. The sequence may contain several non-standard amino acids or other unusual components. Cyclic lipopeptides are typically composed of 11 to 13 amino acid residues, forming a peptide ring, which stabilizes the lipopeptides against proteolysis. The fatty acid chain promotes the insertion of lipopeptides into bacterial membranes.

The fatty acid chain attached at the N-terminus is a key structural feature of lipopeptides. The lipid tails differ remarkably in branching, degree of saturation and oxidation states, contributing to the high structural diversity of this class of antimicrobial agents. Among lipopeptides from natural sources, the lengths of the lipid tails are in the range of 5 to 16 carbons, with the shortest one (5-carbon chain) found in the linear lipopeptide dragomide E [32], and the longest one (sixteen-carbon chain) found in glycinocin B [33]. It has also been demonstrated that a correlation may exist between the fatty acid chain length and the antimicrobial activity and toxicity of these lipopeptides. For example, a study using lipopeptides with different lipid tail lengths (10, 12, 14 or 16 carbons) demonstrated that the antibacterial activity generally decreased with the increase of the length of the lipid tail, while the antifungal activity was higher for larger lipopeptides. In addition, lipopeptides with 10 or 12 carbons in the fatty acid chain seem to be non-hemolytic, whereas the larger ones are hemolytic [34].

1.2.2 Mechanism

Although many efforts have been made to clarify the mode of action of lipopeptides, there is no clear and fully understood mechanism. Some crucial properties have been identified as being essential for their antibacterial activity. Firstly, many lipopeptides tend to form oligomers. For example, tsushimycin forms dimers in its crystal structure, with the help of Ca^{2+}, yielding a large hydrophobic surface facilitating the interaction with the bacterial cell membrane [35]. More evidence includes a direct correlation between oligomerization of the lipopeptides in solution and potent antifungal activity, showing that only lipopeptide oligomers were antifungal [36]. Another key feature of lipopeptides related to their antimicrobial activity is that they can interact with membranes via the lipid acyl chain. Evidence has been demonstrated that for MSI-843, the

interaction between membrane and peptides with two hydrocarbons chains is much stronger than when only one hydrocarbon chain is attached to the lipopeptide [37]. Two main mechanisms of lipopeptides have been proposed [30]: i) inhibition of cell wall synthesis, e.g. inhibition of β-(1,3)-D-glucan or chitin by echinocandins [38]; ii) disruption of cell membrane via non specific channel or pore formation, e.g. surfactin [39]. Previous studies demonstrated that lipopeptides interact with bacterial membranes with the help of the lipid tail, and the insertion into the lipid bilayer introduces defects in the membrane, increasing permeability and causing cell death as a result. Lipopeptides in the second proposed mechanism act in a similar manner to antimicrobial peptides. Similar to AMPs, lipopeptides do not target a receptor in the bacteria specifically, but interact with the bacterial membranes with characteristic lipid compositions, making it difficult for bacteria to develop resistance [40]. Lipopeptides may also disrupt other cellular processes such as DNA replication, transcription and translation.

1.3 Daptomycin

Daptomycin is an acidic lipopeptide antibiotic, composed of 13 amino acid residues, with the N-terminus acylated with an *n*-decanoyl fatty acid chain. It was first developed by researchers from Eli Lilly in the early 1980s by the addition of an *n*-decanoyl side chain to the A21978C core peptide [41]. It became the first clinically approved member of the novel class of lipopeptide antibiotics by the Food and Drug Administration in 2003 for the treatment of severe skin and soft tissue infections caused by Gram-positive pathogens such as *S. aureus* and *E. faecalis* [42]. It is sold under the market name CUBICIN by Cubist Pharmaceuticals. Later in 2006, it was approved for the treatment of bacteremia caused by MRSA [43]. Daptomycin has several features making it an attractive novel antibiotic: broad-spectrum activity against Gram-positive

pathogens including multidrug-resistant species; low frequency of bacterial resistance in clinical cases; rapid killing of bacteria; efficient killing of bacteria in all growth phases including the stationary phase; and it is useful in the treatment of indolent, deep-seated infections [44]. Although there is not yet full agreement among researchers regarding how daptomycin kills Gram-positive pathogens, several features are believed to be necessary for its antibacterial activity. Calcium ion is required for the binding of daptomycin to the membrane, and daptomycin is only active to membranes that contain negatively charged lipids such as phosphatidylglycerol (PG). Daptomycin has attracted interest, as its mode of action is different from other antibiotics on the market. The history of daptomycin development and different mechanisms are presented in Figure 1.3.

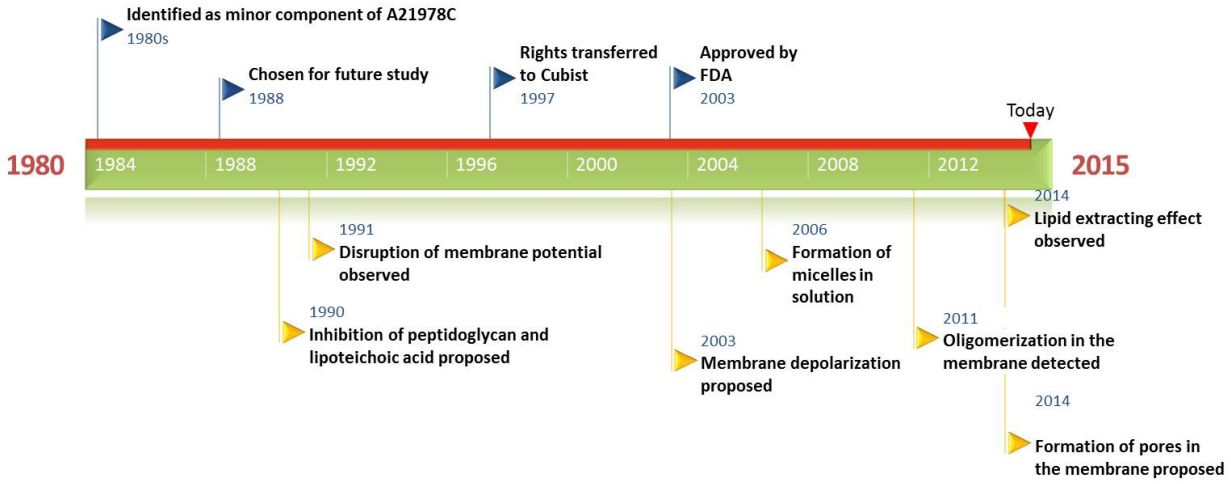

Figure 1.3 Timeline of daptomycin's history and development of different mechanisms.

1.3.1 History and synthesis

Daptomycin was firstly prepared in the 1980s and initially named LY 146032. It was initially isolated as a minor component of the A21978C factors [45], a family of acidic lipopeptide

antibiotics inhibiting Gram-positive pathogens. A21978C is produced via the action of nonribosomal peptide synthetases (NRPSs) in *S. roseosporus* [45], which was originally isolated by scientists at Eli Lilly from a soil sample. All A21978Cs are composed of a common thirteen-amino acid peptide nucleus, but have various fatty acid groups attached to the N-terminus. The peptide core consists of a 10-membered ring. Three major family members, A21978C_{1-3}, are composed of branched fatty acid chains having 11, 12 and 13 carbon atoms, which are found to be *anteiso*-undecanoyl, *iso*-dodecanoyl and *anteiso*-tridecanoyl, respectively. As daptomycin is just one minor component of the A21978C factors, daptomycin is prepared by the reacylation of an *n*-decanoyl side chain to the A21978C core cyclic peptide, which is produced by incubation A21978C with *A. utahensis* to cleave the natural fatty acid side chain from the A21978C factors [46]. The structures of A21978C family members and daptomycin are shown in Figure 1.4. Activity and toxicity of A21978C derivatives is related to different acyl groups [47]. *In vitro* studies against *S. aureus* and *S. pyogenes* showed an increase in antibacterial activity with increasing acyl chain length up to 13 carbons, however *in vivo*, LD_{50} values, showed that analogs with a chain longer than C10 have a trend of increasing toxicity when the acyl chain length is increasing [47]. Among the derivatives, daptomycin showed the best therapeutic index in mice, making it a potent and useful analogue [47].

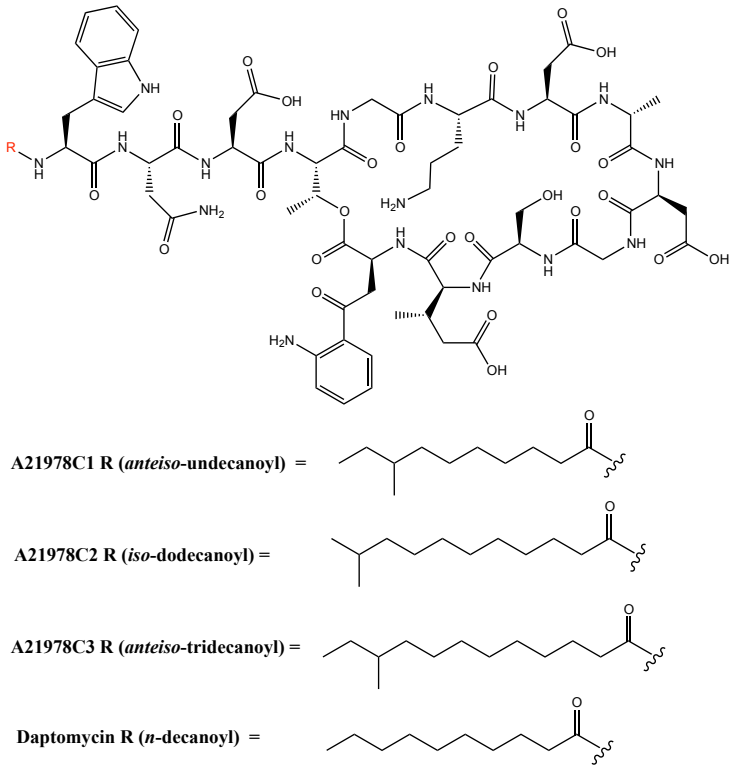

Figure 1.4 The structures of three major A21978C family members and daptomycin.

During the early clinical trials, researchers found that daptomycin caused some adverse effects on skeletal muscle, including myopathy with muscle weakness and elevated serum creatine phosphokinase. Therefore, the development of clinical usage was on hold until 1997, when the rights were transferred to Cubist Pharmaceuticals. Cubist worked on the formulation, leading to the FDA approval of daptomycin in 2003.

At present, daptomycin is obtained in high yield by the fermentation of *S. roseoporus* by adding decanoic acid [48] to the culture medium, rather than the semi-synthetic method used during the earlier work. Fermentation parameters such as cultivation temperature and feeding rates were optimized in order to minimize the toxicity of accumulated decanoic acid to the bacteria. Daptomycin is isolated as the major component through this optimal fermentation process, with a

yield of about 150 mg/L, which simplifies the next purification step. In addition, a number of improvements have been made in daptomycin production using *S. lividans* (TK23 and TK64 strains) [49].

1.3.2 Structure

As mentioned above, daptomycin consists of 13 amino acids. Among the 13 residues include several non-proteinogenic amino acids, which are D-Asn, D-Ala, D-Ser, (2R,3R)-methylglutamate (MeGlu), ornithine (Orn) and kynurenine (Kyn). The sequence of daptomycin is n-decanoyl-Trp-D-Asn-Asp-Thr-Gly-Orn-Asp-D-Ala-Asp-Gly-D-Ser-MeGlu-Kyn and its structure in shown in Figure 1.4. The formation of an ester bond between Thr4 and Kyn13 builds a ten-membered macrolactone ring in daptomycin [45]. Daptomycin has an overall negative charge at neutral pH, with the presence of four carboxylic residues (three aspartic acids, and one methyl-glutamic acid) and two amines (aliphatic amine in ornithine and aromatic amine in kynurenine). The lipid tail of daptomycin is a linear *n*-decanoyl acyl side chain. Daptomycin displays an overall amphipathic structure, with a large number of negatively charged groups and the lipid tail and hydrophobic residues giving it hydrophobicity.

1.3.3 Mechanism

Understanding the mode of action of an antibiotic is crucial for optimized patient care, resistance prevention, infection control and avoiding antagonistic potentials in antibiotic combinations. At this time, the hypothetical mode of action reported consistently for daptomycin includes the calcium-dependent binding to the cytoplasmic bacterial membrane and the oligomerization of

daptomycin in the membrane. However, the detailed mechanism of daptomycin is still not thoroughly understood, although a number of studies have been carried out.

Early studies proposed that the mechanism of action for daptomycin is the inhibition of peptidoglycan [50] and lipoteichoic acid biosynthesis [51], and a decrease in the membrane potential [52]. However, later experimental results showed that the antibacterial activity of daptomycin against *S. aureus* and *E. faecalis* is not related to the inhibition of lipoteichoic acid biosynthesis [53, 54]. In addition, a direct correlation between the membrane potential and growth of *S. aureus* treated with daptomycin is reported [53], supporting that membrane depolarization is the primary mode of action of daptomycin. Furthermore, the formation of oligomers of daptomycin in solution at millimolar concentrations and in the membrane at micromolar concentrations was detected. Finally, studies indicated that daptomycin causes rapid bactericidal activity not involving penetration into the cytoplasm or cell lysis [53, 55]. Therefore it is proposed that the oligomers in the membrane may cause the membrane depolarization by forming ion channels [56] or via a lipid extracting effect [57].

1.3.3.1 Inhibition of peptidoglycan or/and lipoteichoic acid biosynthesis

One of the main mechanisms studied before 2003 is the inhibition of peptidoglycan and/or lipoteichoic acid (LTA) biosynthesis by daptomycin [46, 50, 51, 58]. Early studies reported that daptomycin inhibits the peptidoglycan synthesis, which is a key component of the cell wall for maintaining the structural integrity of the cell. It was also suggested that the inhibition of peptidoglycan synthesis is by interfering with the formation of the peptidoglycan precursor,

UDP-MurNAc pentapeptide [58]. In addition, no strong inhibition of other macromolecules such as protein, RNA, DNA, or lipids by daptomycin was detected [58].

Daptomycin inhibiting peptidoglycan biosynthesis was confirmed in later results, but a significant inhibition occurred only when the daptomycin concentration exceeded the MIC. However, the MIC of daptomycin only inhibited lipoteichoic acid by over 80% at 10 min after antibiotic treatment. This suggests that the target of daptomycin is the inhibition of lipoteichoic acid synthesis [51]. Figure 1.5 shows a schematic of the proposed lipid metabolism in *E. hirae* [59]. After treatment with daptomycin, the accumulation of compound 1 was observed, while the amounts of compounds 2, 3, and 4 decreased meanwhile, indicating a possible site of action of daptomycin [59].

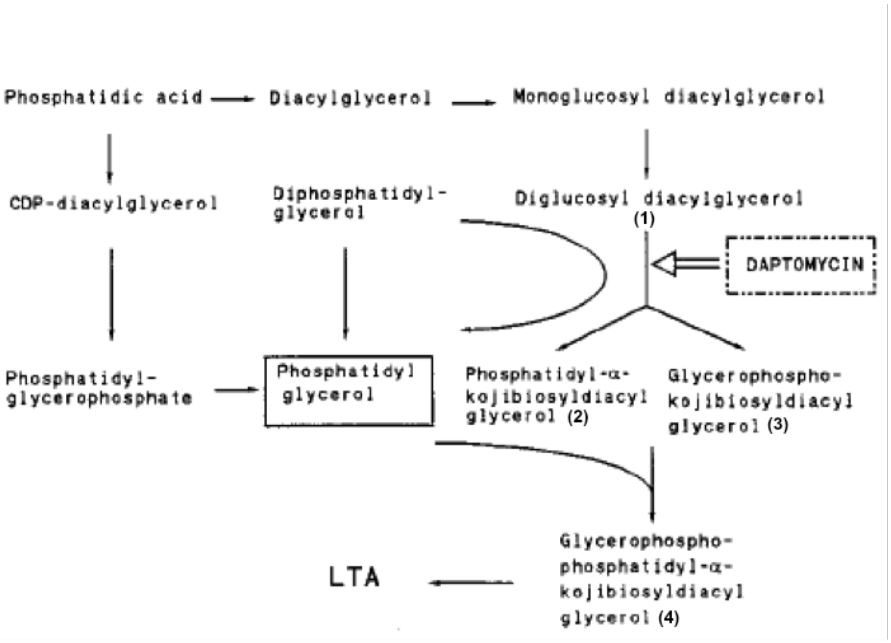

Figure 1.5 The proposed outline of the lipid metabolism in *E. hirae*. Figure adapted from [59].

This mechanism was disputed in 2003 when a study [54] showed that daptomycin was able to inhibit macromolecular synthesis including RNA and lipids in *S. aureus*, *E. faecalis*, and *E. hirae*

and there was no dose or kinetic specificity for lipoteichoic acid. In this investigation, it was also demonstrated that lipoteichoic acid could not be the daptomycin-binding molecule or specific receptor, as the addition of exogenous LTA did not change the MICs of daptomycin significantly. These results indicate that lipoteichoic acid biosynthesis is not the target of daptomycin in these pathogens.

1.3.3.2 Membrane depolarization

Since the mechanism described in section 1.3.3.1 was called into question, an alternative mechanism was required. This mechanism focuses on the membrane depolarization caused by daptomycin. It was observed that daptomycin caused a dissipation of membrane potential in *S. aureus* [52]. Daptomycin is also shown to induce potassium efflux in *S. aureus* and *B. megaterium* [58]. These results suggest that daptomycin can cause ion movements across the cell membrane, followed by collapse of the transmembrane electrical potential gradient, a process termed depolarization [60]. A correlation between the initial rate of release of potassium from daptomycin-treated cells and the loss of cell viability was then reported [53], supporting the hypothesis that bactericidal activity of daptomycin is mediated by membrane permeabilization and depolarization. In addition, flow cytometric assays also showed that cell viability decreases in parallel with the changes in membrane potential [53]. So a revised model was proposed based on this report and other published results, as shown in Figure 1.6 [61]. Daptomycin binds and inserts into the cytoplasmic membrane in a calcium-dependent manner via its lipid tail, followed by the formation of daptomycin oligomers, which is also supported by some recent experiments [62, 63]. This leads to the formation of ion channels or larger nonspecific pores (see also Chapter 3). The formation of these structures disrupts the integrity of the membrane and allows efflux of

potassium, leading to depolarization of the membrane. Accompanied with membrane depolarization, bacterial cells may lose the ability to accumulate substrates or synthesize macromolecules, leading to rapid cell death.

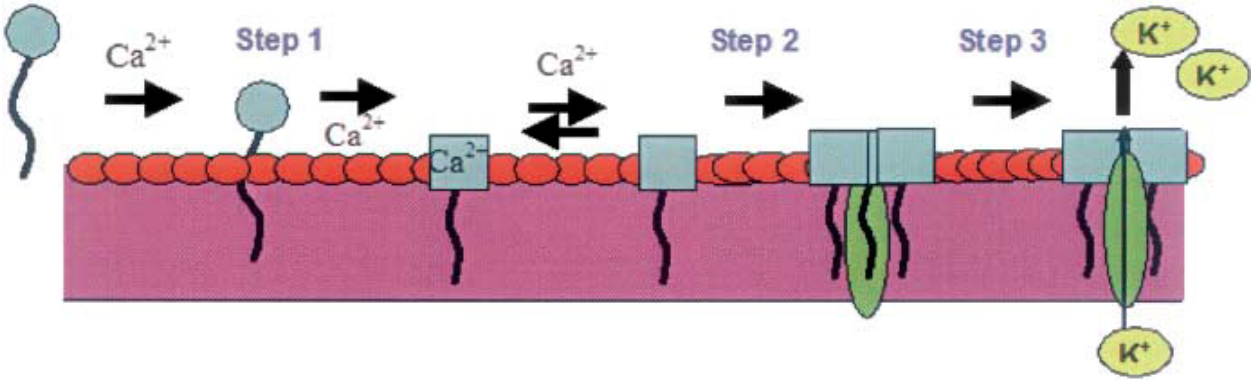

Figure 1.6 Hypothetical mechanism of action of daptomycin. Daptomycin inserts into the bacterial membrane via its lipid tail in the presence of Ca^{2+}, followed by the formation of daptomycin oligomers in the membrane, leading to the leakage of intracellular ions and cell death. The figure is adapted from [61].

Nonetheless, depolarization is not lethal to the bacterial cells. Valinomycin is found to be bacteriostatic, but has the ability to cause depolarization [64]. In addition, some researchers found that in non-growing cells, cell death precedes membrane depolarization, suggesting that depolarization may not be the direct cause of cell death under these conditions [65]. Therefore, the mechanism of action of daptomycin may be more complex than just causing membrane depolarization. Additional effects of daptomycin may include damaging membrane integrity, inhibition of protein, DNA, RNA and lipoteichoic acid synthesis.

1.3.3.3 Interaction with divalent ions

Although the details of mode of action of daptomycin are not clear, it is agreed among researchers that daptomycin requires the presence of physiological levels of calcium ions for antimicrobial activity. Calcium ions are believed to facilitate the insertion of daptomycin into the bacterial cytoplasmic membrane. Calcium ions act as a bridge between the negatively charged amino acid residues on daptomycin and the negatively charged phospholipids that are typical components of the cytoplasmic membrane of Gram-positive bacteria, thereby allowing for deeper insertion of daptomycin into the membrane.

To obtain a better perspective of this calcium-dependent binding, structures of daptomycin in apo-form and with calcium ions conjugated have been solved. It was suggested that the binding of calcium to the daptomycin caused a conformational change that increased its amphipathicity based on NMR spectra [65]. However, the occurrence of this conformational transition has been questioned by the finding that divalent ions such as calcium and magnesium ions promote the formation daptomycin micelles [66]. In addition, the structure of daptomycin does not change significantly in the presence of lipids and Ca^{2+}, based on NMR experiments [67].

1.3.3.4 Oligomerization in solution and in the membrane

As mentioned in section 1.3.3.3, daptomycin has been found to form micelles in the presence of 1 or more equivalents Ca^{2+} in aqueous solution, with an aggregation number of 14 – 16 [66, 68, 69]. The arrangement into micelles is believed not to be accompanied by a conformational change of daptomycin.

It has been demonstrated that any two of the four acidic amino acid residues, Asp3, Asp7, Asp9 and MeGlu12 in the apo-form daptomycin, are not in close proximity spatially so as to serve as a Ca^{2+}-specific binding site without a major conformational change. The formation of micelles is suggested to be favored by either π-stacking interactions between aromatic residues in different daptomycin molecules or the arrangement of the lipid tails facing the inside of the micelle, where Ca^{2+} would be at the interface between daptomycin molecules due to the electrostatic interactions [66].

The daptomycin micelles are proposed to dissociate when close to the membrane, allowing daptomycin insertion into the membrane. It is suggested that another oligomerization step may occur in the membrane. Daptomycin disturbs membranes by inducing positive curvature strain on the membrane, in the presence of Ca^{2+}, as shown from differential scanning calorimetry and solid state ^{31}P NMR data [70]. Thus daptomycin oligomers are predicted to form ion channels, disrupt the bacterial membrane and induce an efflux of intracellular ions, indicating the calcium-induced daptomycin aggregates formed in the membrane are necessary for its bactericidal activity. The formation of daptomycin micelles is presented in Figure 1.7.

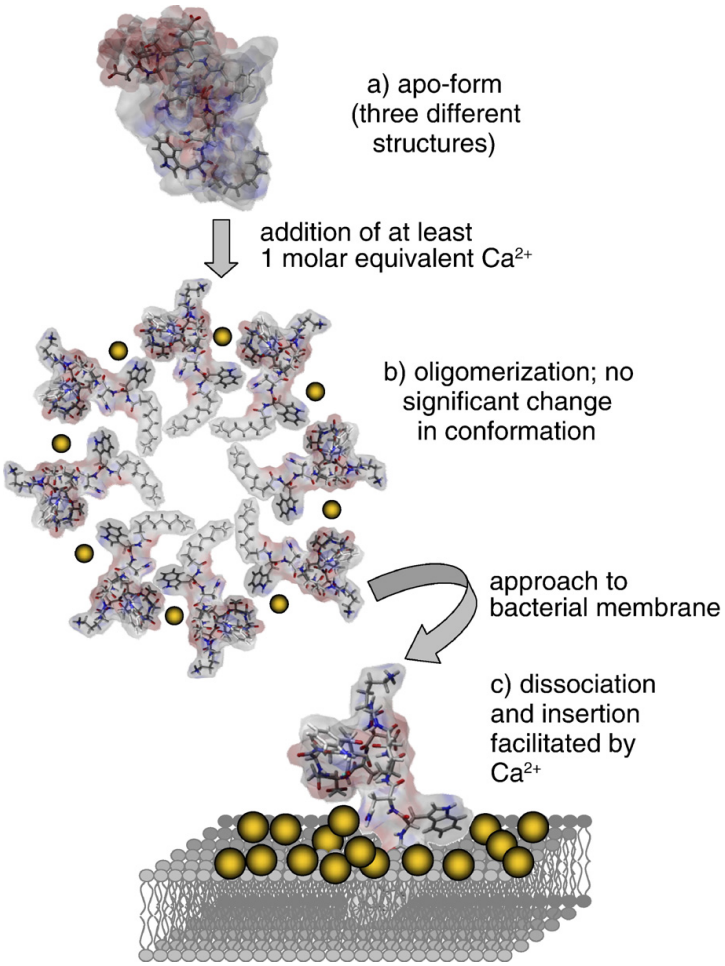

Figure 1.7 The revised model that takes micelle formation in aqueous solution into account. Figure is adapted from [67].

Although the idea of forming daptomycin oligomers in the membrane has been postulated for a long time, experimental evidence has only been recently available. Muraih et al. [62] have investigated the oligomerization of daptomycin in the membrane using fluorescently labeled and functionally active daptomycin derivatives. Daptomycin oligomers formed on liposome membranes containing phosphatidylglycerol (PG) were identified through Förster resonance energy transfer (FRET) and self-quenching of NBD fluorescence. The requirements for oligomerization to be observed are similar to those for membrane permeabilization and

bactericidal activity [10, 47], indicating that the membrane depolarization may be caused by the daptomycin oligomer. Daptomycin oligomerization in the membrane was further characterized through excimer fluorescence using perylene-daptomycin, i.e. the fatty acyl chain was replaced with perylene-butanoic acid. Under the conditions used in the previous FRET experiments, excimer fluorescence was observed, indicating that fatty acyl residues of perylene-daptomycin of the membrane-associated oligomer are close to each other. Thus the formation of daptomycin oligomers in both liposomes and bacterial cells [63] was supported. Moreover, the subunit number of daptomycin oligomers on the membrane was estimated by FRET was found to be about 6-7 subunits [71] (more discussion on this point in Chapter 2). It was also suggested that oligomerization is indeed required for antibacterial action of daptomycin by investigating hybrid oligomers of daptomycin and CB-182,462, a semisynthetic derivative of A54145 that shares substantial structural similarity with daptomycin [72]. If the two antibiotics act independently on the target using the same mode of action, their mixtures should display an additive antibacterial effect. But for the hybrid oligomers, the MIC is greater than additive dosages, indicating that the two drugs inhibit each other and oligomerization in the membrane is important for antibacterial function. On the other hand, the impaired antibacterial activity of the hybrid oligomers indicates that oligomer formation is not sufficient but a subsequent step is required for killing bacteria. Thus daptomycin and CB-182,462 can form oligomers but their differences in structure prevent subsequent steps in the mechanism, leading to cell death.

1.3.3.5 Formation of ion channels or pores

In order to investigate the permeability of the membrane caused by daptomycin, additional *in vivo* and *in vitro* studies have been performed using other ions such as Na^+ and larger molecules

such as ATP and proteins. The results demonstrated that potassium is not the only intracellular component that is released after the cells are treated with daptomycin. Indeed, loss of magnesium and ATP is accompanied by the leakage of potassium and membrane depolarization [73]. In daptomycin-exposed *B. anthracis*, sodium influx was also observed [74], further supporting the finding that other components can also go through the membrane. Although a previous study suggests that leakage of ATP occurs, most researchers believe that daptomycin only causes release of ions, including K^+ and Mg^{2+} [55, 57, 73]. The loss of these two ions starts after 10 min of exposure to daptomycin at a similar rate [73].

As mentioned before, bacterial cells undergo membrane depolarization after treatment with daptomycin, suggesting that channels or pores are formed in the target membranes [53]. Unlike AMPs, which can cause pore formation in the membrane and leakage of molecules, daptomycin is expected to differ from the mechanism of AMPs. Zhang et al. [56] detected and characterized the permeability properties of the membrane pores caused by daptomycin by using a liposome model system. From their results, they concluded that the pores are selective for cations, with a higher permeability for Na^+, K^+ and other alkali metal ions. The permeability for Mg^{2+} was found to be about twice smaller. The permeabilities are even lower for the organic cations choline and hexamethonium ($C_{12}H_{30}N_2$), while anions and the zwitterion cysteine are excluded. Interestingly, however, the movement of ions across the membrane was only observed when both daptomycin and the proton ionophore carbonyl cyanide *m*-chlorophenyl hydrazine (CCCP) were added together. For known ion channel-formation peptide aurein 2.3, CCCP is definitely not required for the translocation of sodium and potassium ions. This will be discussed further in Chapter 3.

1.3.3.6 Lipid extracting effect

Although the leakage of ions caused by daptomycin was observed (refer to section 1.3.3.5), the effect was different from ubiquitous membrane-acting AMPs, suggesting that membrane pores may not be formed. Another possible effect that explains how daptomycin affects the permeability of the membrane is called the lipid extracting effect, which was presented recently [57]. In this model, daptomycin removes lipid molecules from giant unilamellar vesicles (GUVs) by forming lipid-peptide aggregates, as shown in Figure 1.8A [57]. The lipid extracting effect caused by daptomycin is observed in the presence of Ca^{2+} and when the GUV contains PG, the same conditions that are required for daptomycin to be active against pathogens. In addition, the lipid extracting effect is dependent on the concentration of daptomycin, as demonstrated in Figure 1.8B, with a threshold concentration of daptomycin, which is similar to the MIC, suggesting that a correlation may exist between the lipid extracting effect and the antibacterial activity of daptomycin. The authors argued that the lipid extracting effect induced by daptomycin could cause water pore defects in the membrane, allowing ion permeation [75]. Thus it is reasonable to expect that lipid extraction can induce the permeabilization of the membrane. The absence of molecular leakage can also be explained since the water pore defects would be so transient and small that molecules cannot travel across the membrane.

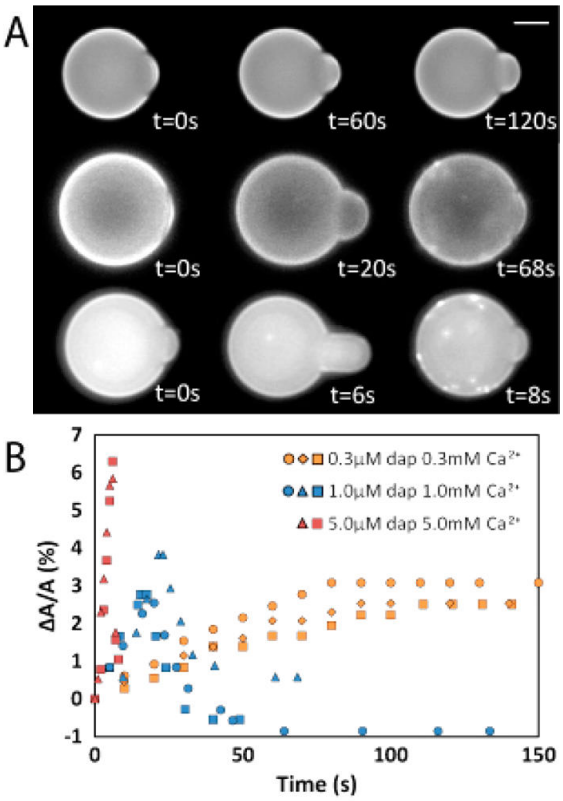

Figure 1.8 Effect of daptomycin at different concentrations on DOPC/DOPG GUVs (including 1% Rh-PE) in the presence of Ca^{2+}. The binding of daptomycin to a GUV can be determined by the expansion of the membrane area. (A) Rh-PE fluorescence widefield images of GUVs aspirated with micropipettes after treatment with different concentrations of daptomycin, i.e. 0.3, 1.0, and 5.0 μM from top to bottom, respectively. For the GUV treated with 0.3 μM of daptomycin, the protrusion length of the GUV into the micropipette increased to a maximal value. While when the daptomycin was at 1.0 or 5.0 μM, the protrusion length increased firstly but then decreased. When the protrusion length decreased, aggregates appeared on the GUV surface (brighter spots on images at t = 68 s and t = 8 s). The scale bar is 10 μm. (B) Fractional area change ΔA/A of the GUVs over time. Figure is adapted from [57].

1.3.3.7 Targeting on cell membrane or cell wall

Although most of the recent studies have focused on the interaction between daptomycin and the cell membrane, the question of whether daptomycin targets the cell membrane, the cell wall or both is not yet solved. Recent studies indicate that modifications of both the cell membrane and the cell wall of the bacteria promote daptomycin resistance [76]. Cell wall has been predicted to be an potential target of daptomycin, supported not only by early studies indicating that daptomycin can inhibit synthesis of peptidoglycan and lipoteichoic acid (see section 1.3.3.1), but also by transcriptional profiling studies showing that daptomycin can induce cell wall stress responses in *S. aureus* and *B. subtilis* [77]. In addition, perturbations and a thickening of the cell wall have been identified in daptomycin resistant strains. On the other hand, modifications of the cell membrane are also identified in daptomycin-resistant strains, including altered cell membrane order, resistance to cell membrane depolarization, and reduced binding of daptomycin [78-80].

A new revised model links two previously separate lines of the proposed the mechanisms of daptomycin. Pogliano et al. observed the interaction between daptomycin and the Gram-positive bacteria *B. subtilis* directly by using fluorescence microscopy [81]. The first observable cellular effects of daptomycin on the cells are the formation of randomly positioned membrane patches. The appearance of the patches precedes the collapse of membrane integrity and cell death by over 30 min. The occasional protuberances on the surface of the MSSA bacteria were also observed after 1 hour treatment of daptomycin from scanning electron micrographs [82]. Daptomycin-induced membrane patches have shown the capability of specifically recruiting the conserved cell division protein DivIVA. Sublethal doses of daptomycin induce membrane

defects and dramatic changes in cell shape, which is determined by the cell wall. There is also a correlation between the membrane patches and the mislocalization of the peptidoglycan synthesis machinery. Therefore, at sub-MIC doses, membrane defects colocalize with DivIVA, fluorescently labeled daptomycin, and fluorescent reporters of peptidoglycan biosynthesis. This suggests a mechanism where daptomycin has a primary effect on cell membranes, with the recruitment of the DivIVA protein, which involves cell division and cell wall synthesis, leading to changes in cell morphology and membrane defects. When daptomycin is at supra-MIC doses, the extent of membrane curvature exceeds the ability of the cell to respond to this change. In this case, discontinuities in the membrane are formed where daptomycin inserts, leading to leakage of ions and membrane depolarization. The revised mode of action of daptomycin at different concentrations is shown in Figure 1.9.

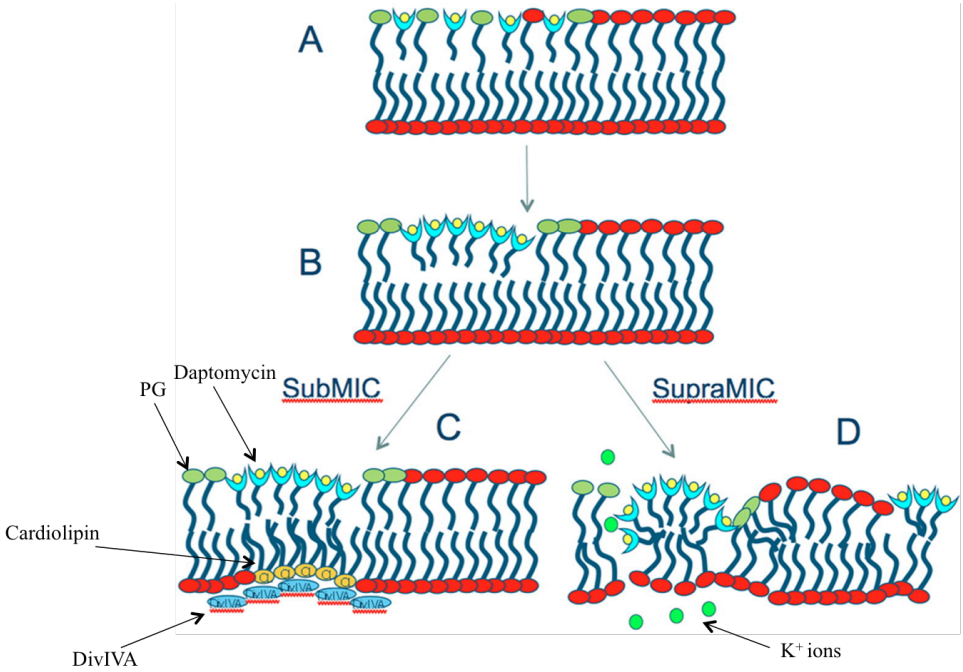

Figure 1.9 A revised model for the mechanism of daptomycin. Daptomycin molecule is the lightblue "cup" with a yellow circle and a tail; PG is in lightgreen; cardiolipin is in yellow; potassium ion is in green; and DivIVA is in blue. Figure is adapted from [81].

1.3.4 Research objectives

Although the formation of daptomycin oligomers in the membrane and its involvement in antimicrobial activity has been recently demonstrated based on recent FRET experiments (see details in section 1.3.3.4), the conditions used for the experiments and the assumptions made to interpret the data may not be valid. In particular, the interpretation of the FRET results does not take into account that daptomycin can cause fusion under conditions similar to those used in the FRET experiments [65]. Not only the formation of oligomers in the membrane but also the membrane fusion can lead to the closer proximity of donors and acceptors, causing FRET to be observed. Taking this consideration into account, we carried out several experiments in Chapter

2 to determine whether fusion plays a role and what impact it plays in the interpretation. I firstly determined the conditions under which daptomycin can cause fusion in the presence of different kinds of lipids and various concentrations of Ca^{2+}, using photon correlation spectroscopy (PSC). Based on the findings of membrane fusion caused by daptomycin, binding and kinetics experiments were conducted to study the interaction between daptomycin and lipid membrane, and Förster resonance energy transfer (FRET) experiments, under conditions where fusion is not present.

In a subsequent study performed by Palmer and co-workers, the ion permeability of daptomycin on model membranes was tested. As mentioned above, these studies made use of a proton ionophore CCCP (refer to section 1.3.3.5 for details). In Chapter 3, fluorescence experiments were conducted in order to investigate the ion permeability property of daptomycin on POPC/PG and DMPC/PG liposomes with or without CCCP. Experiments using the ion-selective pore-forming aurein peptide were also done as a control.

The impact of our findings on the mechanism of action of daptomycin will be summarized in Chapter 4, along with suggested future experiments to elucidate how daptomycin works.

Chapter 2: Concentration effects: Implications on the mechanism of action of daptomycin

2.1 Introduction

As mentioned in Chapter 1, a large number of studies on mode of action have proposed the involvement of daptomycin oligomers in the membrane as an important step in the killing mechanism of daptomycin. Recent Förster resonance energy transfer (FRET) experiments, performed by Muraih et al. [62, 71], have finally shed light on the question. FRET between a native daptomycin (acts as the donor) and an NBD-labeled daptomycin derivative (acts as the acceptor) was observed in the presence of Ca^{2+} using model membrane systems containing the negatively charged phosphatidylglycerol (PG) and membrane vesicles isolated from *B. subtilis* [62]. The absorbance and fluorescence emission spectra of native daptomycin and NBD-daptomycin are shown in Figure 2.1. NBD-daptomycin has an absorbance peak at 475 nm overlapping the emission peak of native daptomycin. When the excitation is at 365 nm and there is FRET between the two fluorophores, the fluorescence emission peak of the native daptomycin will decrease and the emission peak of the NBD-daptomycin will increase. Since FRET occurs when the donors and acceptors are in close proximity, Muraih et al. concluded that oligomerization of daptomycin was firstly detected based on the observed FRET. In a later study, Muraih et al. estimated the subunit number of the membrane-associated daptomycin oligomer by FRET [71]. It was suggested that the oligomerization number is approximately 6 to 7, or twice if the oligomer interacts with both membrane leaflets. A revised mechanism of action of daptomycin was proposed, as illustrated in Figure 2.2. In this mode of action, daptomycin firstly

inserts into the membrane containing PG with the help of Ca^{2+} and then forms daptomycin oligomers with the subunit number of 6-7 [71], leading ultimately to leakage of intracellular ions.

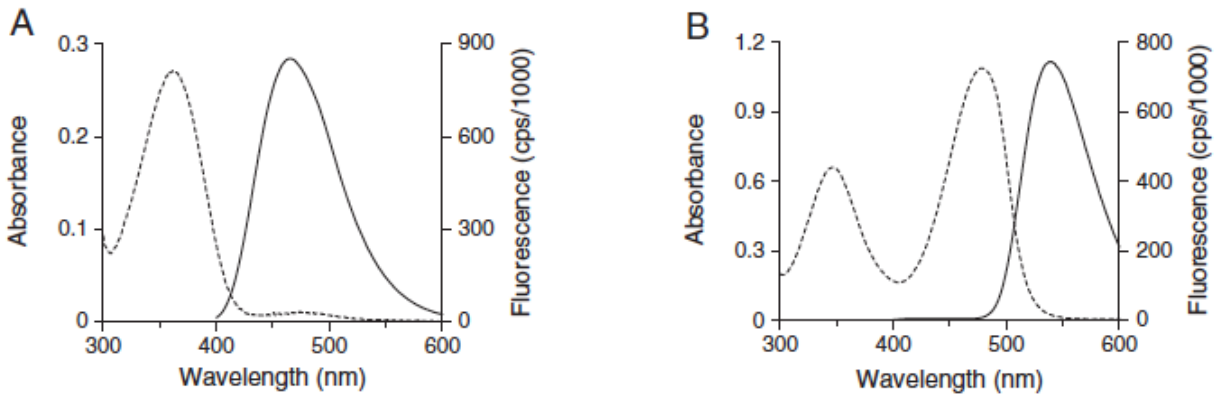

Figure 2.1 Absorbance (dashed lines) and fluorescence emission (solid lines) spectra of A) daptomycin and B) NBD-daptomycin. The figure is adapted from [62].

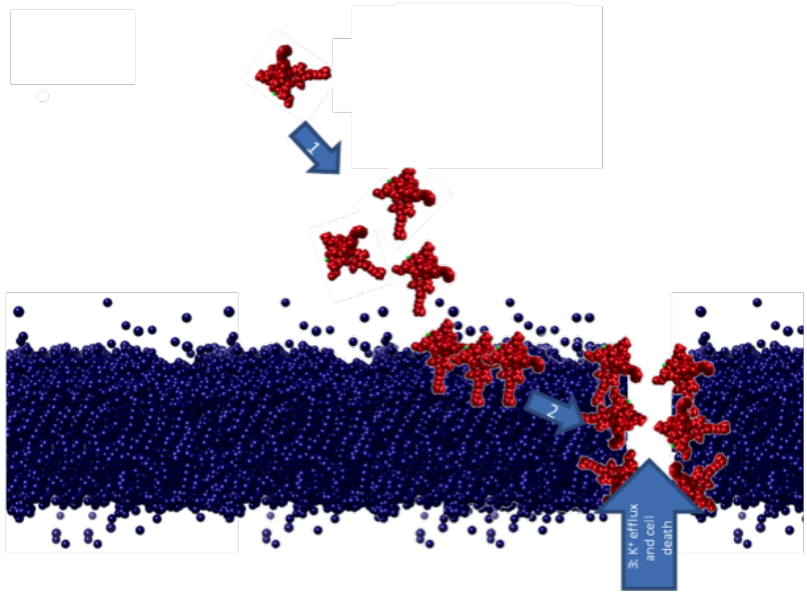

Figure 2.2 Mechanism of action of daptomycin on the basis of recently published FRET results [62, 71]. Refer to the text for a detailed description of the steps. Figure adapted with slight modifications from J. Zhang W.R.P. Scott, F. Gabel et al., manuscript under revision.

A number of assumptions were made in this membrane-bound model including that: i) all of the daptomycin interacts with the lipid bilayer membrane; ii) daptomycin forms only one type of oligomer in the membrane, with the same number of subunits, n; iii) the fluorescence measured only comes from oligomers containing daptomycin only, but not NBD-labeled daptomycin; and iv) daptomycin does not cause membrane fusion in the presence of calcium. In Figure 2.3, the curves representing the theoretical number of oligomer subunits are calculated according to the following equation:

$$D = \frac{d^n}{d} = d^{n-1} \text{ (Eq. 2.1)}$$

where d is the fraction of daptomycin in a original mixture with NBD-daptomycin. After oligomers have been formed according to assumptions 2 and 3, the fraction of oligomers that are composed of only native daptomycin without NBD-daptomycin will be d^n. D represents the fraction of native daptomycin from the mixture that contribute to the formation of these oligomers containing only daptomycin, which equals to the relative kynurenine fluorescence [71].

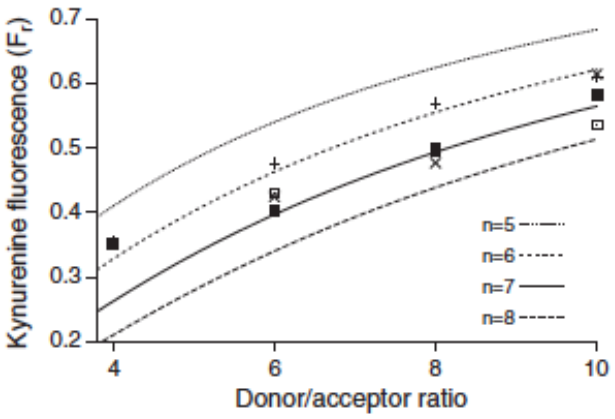

Figure 2.3 Determination of oligomer subunit stoichiometry by FRET. Kynurenine fluorescence intensities were measured using four different donor/acceptor ratios, and each ratio is repeated four times. The curves representing the theoretical subunit number n obtained from Eq. 2.1. Figure adapted from [71].

FRET occurs typically when the distance between the donor and the acceptor is within 1 – 10 nm. The formation of oligomers composed of donors and acceptors can be a reason leading to FRET from the unlabeled to the labeled daptomycin molecules. However, membrane fusion can also cause an increase in FRET efficiency, since the donor and acceptor in the separate vesicles can be in close contact when fusion occurs. The process of membrane fusion is shown in Figure 2.4. Although membrane fusion may not be an important factor *in vivo*, due to the presence of the peptidoglycan layer found on the outside membrane in Gram-positive bacteria, it is likely to be significant when interpreting data from *in vitro* experiments. If fusion occurs, it becomes difficult to conclusively say that FRET only arises from oligomerization within a lipid bilayer since fusion can also lead to FRET. The obtained subunit number may mean that 6-7 daptomycin molecules are required to drag two membranes into close contact for fusion to occur.

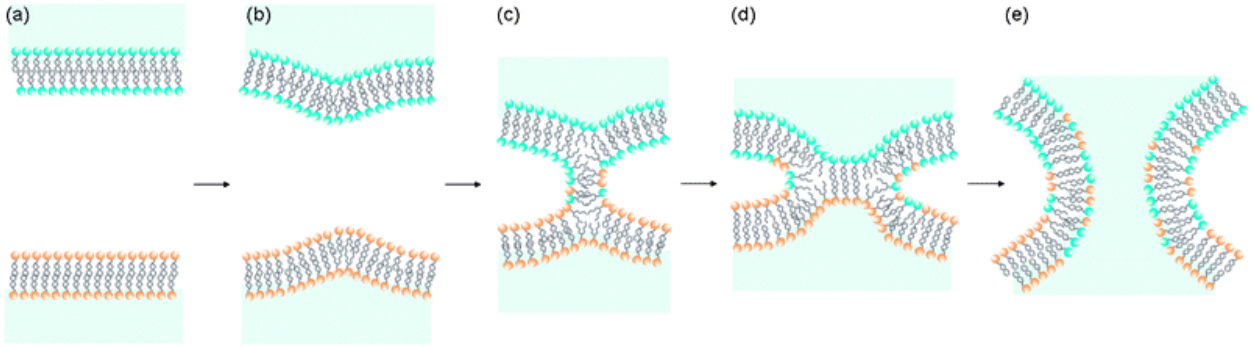

Figure 2.4 Proposed steps of membrane fusion. (a) Membrane lipid bilayers are brought into reasonably close contact by some fusion machinery. (b) A point-like membrane protrusion is formed to reduce the energy of the repulsion between the leaflets of the membranes coming into immediate contact. (c) A hemifusion stalk with proximal leaflets fused. (d) Stalk expansion leading to hemifusion. (e) A fusion pore is formed. The figure is adapted from [83].

Several experiments were performed to acquire a better understanding of the impact of fusion on the interpretation of the FRET data. We firstly determined the conditions under which daptomycin can cause fusion in the presence of different kinds of lipids and various concentrations of Ca^{2+}, using photon correlation spectroscopy (PSC). Based on the results of membrane fusion caused by daptomycin, we then conducted binding and kinetics experiments to study the interaction between daptomycin and lipid membrane, and FRET experiments, under conditions where fusion is not present. Finally, our results are discussed on the basis of proposed mechanisms of action of daptomycin.

2.2 Materials and methods

2.2.1 Materials

Daptomycin was a generous gift of Cubist Pharmaceuticals (Lexington, MA, USA). 1-palmitoyl-2-oleoyl-*sn*-glycero-3-phosphocholine (POPC), 1-palmitoyl-2-oleoyl-*sn*-glycero-3-phospho-(1'-

rac-glycerol) (POPG), 1,2-dimyristoyl-d54-*sn*-glycero-3-phosphocholine (DMPC), 1,2-dimyristoyl-*sn*-glycero-3-phospho-(1'-rac-glycerol) (DMPG), 1',3'-bis[1,2-dimyristoyl-*sn*-glycero-3-phospho]-*sn*-glycerol (CL) were purchased from Avanti Polar Lipids, Inc. (Alabaster, AL, USA). 4-Chloro-7-nitrobenzofurazan (NBD-Cl), 4-(2-hydroxyethyl)piperazine-1-ethanesulfonic acid (HEPES) and acetonitrile were purchased from Sigma-Aldrich (St. Louis, MO, USA). Sodium borate buffer (0.5 M, pH 8.0) was obtained from Alfa Aesar (Ward Hill, MA, USA). Acetic acid was purchased from Fisher Scientific (Nepean, ON, Canada). Ammonium acetate and ethylenediaminetetraacetic acid (EDTA) were purchased from Fisher Scientific (Fair Lawn, NJ, USA).

2.2.2 Preparation of NBD-daptomycin

NBD-labeled daptomycin was prepared as outlined in [62]. Briefly, daptomycin (0.6 mM) was dissolved in 50 mM sodium borate buffer containing 20 mM EDTA, pH 8.0. NBD-Cl solution (25 mM) was prepared in acetonitrile. To 15 ml of the daptomycin solution, 5 ml of NBD-Cl solution was added in a round-bottom flask. The reaction solution was stirred at 60 ˚C for 5 hours in an oil bath and then cooled down in an ice water bath for 2 min. 20 mL of acetic acid (50 mM) was added into the reaction mixture to terminate the labeling reaction.

The crude product was purified using semi-preparative HPLC on a Waters 600 system (Waters Ltd., Mississauga, ON, Canada) equipped with Waters 2996 Photodiode Array Detector. The separation was performed on a Phenomenex C18 reversed-phase column (250 mm × 21.2 mm) using a mobile phase consisting of acetonitrile and 20 mM ammonium acetate (pH 5.5) at a flow rate of 10 ml/min. The gradient started at 30% acetonitrile, rose to 40% in 5 min, and then was

kept constant until the 35 min time point. Factions were collected and identified by spectrophotometry, fluorescence spectroscopy and mass spectrometry. The molecular weight of the purified NBD-daptomycin determined by MALDI-TOF was 1783.9 g/mol, in agreement with the calculated molecular weight of 1783.77 g/mol.

2.2.3 Photon correlation spectroscopy

Samples were prepared using the lipid mixtures, as described in the results section. Vesicles were prepared by evaporating the organic solvent under a dry nitrogen stream. The resulting lipid film was thoroughly dried under vacuum overnight. Then the lipid film was hydrated in 20 mM HEPES buffer (pH 7.5) to a final total lipid concentration of 260 μM. After five freeze-thaw cycles, the lipid suspension was extruded 10 times through two stacked 50 nm polycarbonate filters, using a nitrogen-pressurized liposome extruder.

The sizes of LUVs were determined using a Beckman Coulter N4 plus particle size analyzer (Mississauga, ON, Canada). Daptomycin or NBD-daptomycin and $CaCl_2$ were added to the extruded liposomes to reach final concentrations, as specified in the results section. The sizes of vesicles were measured using 600 nm laser light at 90˚ after incubation of the samples for 15 min at 23 ˚C.

2.2.4 FRET experiments

Fluorescence emission spectra were obtained on a Tecan Infinite M1000 fluorescence plate reader (Morrisville, NC, USA). Samples were composed of HEPES buffer (20 mM, pH 7.5), extruded liposome (260 μM total lipid), $CaCl_2$, and either daptomycin or NBD-daptomycin alone or together in different proportions and concentrations. In the premixed samples, daptomycin and

NBD-daptomycin were mixed before adding the membranes and calcium. In the sequential samples, a solution containing daptomycin, calcium and membranes was incubated for 30 min before addition of NBD-daptomycin. The excitation wavelength was 365 nm, and emission was recorded from 400 to 600 nm. Bandwidths for excitation and emission were 5 nm.

2.2.5 Binding isotherms

Binding experiments of peptides to LUVs were performed by measuring fluorescence spectra with the successive addition of different concentrations of liposomes. Appropriate aliquots of a concentrated DMPC/DMPG or POPC/POPG (1:1) stock solution (6.5 mM) were added to a 2 ml daptomycin solution (4 μM) containing 420 μM Ca^{2+} in HEPES buffer (20 mM, pH 7.5). These concentrations were chosen in order to ensure that fusion between liposomes was avoided. The solution was kept under constant magnetic stirring for 5 min to reach equilibrium after each addition of liposomes. Fluorescence spectra were measured on a Perkin Elmer LS50B luminescence spectrometer. The emission spectra were recorded from 400 nm to 600 nm with the excitation wavelength of 365 nm, using emission and excitation slit widths corresponding to a 5 nm bandwidth. Both kynurenine and NBD fluorescence intensity increased upon binding of daptomycin to liposomes. This binding behavior was analyzed using two models: i) partitioning of the daptomycin into the lipid phase; and ii) apparent binding of the daptomycin to the liposomes. Since excess Ca^{2+} is present in these experiments, only an equilibrium between free and bound daptomycin is taken into account in the models.

Fluorescence measurements were used to determine partition coefficient, K_p, using the following formula [84]:

$$X_b = K_p C_f \qquad \text{(Eq. 2.2)}$$

where X_b represents the molar ratio of bound peptide to total liposome and C_f denotes the equilibrium concentration of the unbound peptide. To determine X_b and C_f, the fraction of the membrane bound peptide f_b was calculated employing the following formula [84]:

$$f_b = \frac{F - F_0}{F_{\max} - F_0} \qquad \text{(Eq. 2.3)}$$

where F_0 is the fluorescence intensity of free peptides in buffer, F is the measured fluorescence intensity, and $F_{\max}$ is the fluorescence intensity when all the peptides are bound to liposomes. The plateau fluorescence signal was considered as $F_{\max}$. Knowing the fraction of bound peptide f_b, the C_f and X_b values could be calculated to obtain the isotherm curve. In practice, X_b was divided by a correction factor of 0.6 since it was assumed that peptides were initially bound to the outer leaflet of the LUV (60% the total lipids) [85]. The partition coefficients were determined from the initial slopes of binding isotherm curve [85, 86].

An apparent dissociation constant K_d was calculated from the plot of f_b against the liposome concentration using the following formula, assuming that the concentration of bound lipid is negligible compared to the total lipid so that the free lipid concentration is close to the total lipid concentration [87]:

$$f_b = \frac{[lipid_{total}]}{K_d + [lipid_{total}]} \qquad \text{(Eq. 2.4)}$$

In this analysis, the peptide is treated as though it binds to discrete sites associated with the liposomes according to the reaction below, where $K_d = k_{-1}/k_1$:

$$\text{Dapto} + \text{Lipid} \underset{k_{-1}}{\overset{k_1}{\rightleftharpoons}} \text{Dapto} \cdot \text{Lipid} \quad \text{(Eq. 2.5)}$$

Note that K_d and K_p are not equivalent.

2.2.6 Kinetics

To generate progress curves for binding of peptide to liposomes, a time-series of fluorescence images were obtained using Olympus IX83 inverted epifluorescence microscope equipped with a 4×/0.16 (magnification/numerical aperture) objective lens, a 120XL X-Cite metal-halide light source and an sCMOS camera (ORCA-Flash4.0, Hamamatsu Photonics, Hamamatsu, Japan). The fluorescence filter combination for daptomycin (kynurenine) fluorescence was a 350/20x excitation filter and a 460/50M band-pass filter (center wavelength/bandwidth; Chroma, Bellows Falls, Vermont, USA). The fluorescence filter combination for band-pass filter for NBD-daptomycin was a 450/20x excitation filter and a 540/50M band-pass filter. A time-series of 100 images was acquired at 0.58 s or 0.66 s intervals to detect the increase in the fluorescence of the kynurenine or NBD after the addition of lipid, respectively. Daptomycin and Ca^{2+} were premixed in a 96-well microtiter plate and the lipid was added after 17 images were taken. Two daptomycin concentrations were tested: 1.44 μM and 3.36 μM (volume = 17.5 μl), with the corresponding Ca^{2+} final concentrations of 180 μM and 420 μM, respectively (volume = 35 ul). These concentrations were used in order to ensure that no fusion occurred between liposomes. The final concentration of lipid is 260 μM, and the volume is 47.5 μl. Each concentration was

repeated three times. After the image acquisition, the images were exported using MetaMorph software (Molecular Devices, Sunnyvale, CA, USA) and analyzed in ImageJ software (National Institutes of Health, Bethesda, MD, USA). The fluorescence intensity was plotted as a function of time and the data fitted using the following function, which relates the intensity to the concentration of bound peptide, C_b, via Eq. 2.5 and the K_d values obtained above:

$$C_b(t) = \frac{F(t) - F_0}{F_{eq} - F_0} f_b(C_b + C_f) \qquad \text{(Eq. 2.6)}$$

where F(t) is the fluorescence intensity measured at time t, F_0 is the baseline fluorescence intensity before adding lipid, F_{eq} is the fluorescence intensity once equilibrium has been reached, and f_b is the fraction of peptide bound to lipid at equilibrium (as calculated from the determined K_d). The fluorescence data was fit with an empirical biexponential growth function, $C_b(t) = f \times (1 - a_1 \times e^{-b_1(t-t_0)} - (1 - a_1) \times e^{-b_2(t-t_0)})$, to permit calculation of an initial binding rate via the first derivative with t set to t_0. A rate constant was then estimated using the equation below, by substituting the initial concentrations of peptide and lipid, and the calculated initial rate at time, t_0.

$$\text{Rate} = k[\text{Dapto}][\text{Lipid}] \qquad \text{(Eq. 2.7)}$$

Finally, the same kinetic data was analyzed using KinTek Eplorer software (KinTek Corporation, Austin, TX, USA). This software analyzes reaction progress data using numerical integration of rate equations derived from a reaction model (Eq. 2.5). This approach was used to recalculate K_d, assuming the simple binding equilibrium above within knowledge of the initial concentrations of peptide and lipid.

2.3 Results and discussion

2.3.1 Binding of daptomycin to the membrane

The binding of daptomycin to model membrane system was determined by two methods, based on the vesicle-induced increase in the fluorescence intensity of kynurenine in daptomycin. The dissociation and partition constants for daptomycin and NBD-labeled daptomycin are listed in Table 2.1. Moreover, rates of binding are given in Table 2.2 for both daptomycin and NBD-daptomycin. The data indicates that binding is strong and, for a system composed of 4 μM daptomycin in about 250 μM lipids, it is reasonable to expect nearly all of the daptomycin to be bound with the lipid bilayers. Interestingly, the binding in DMPC/PG vesicles seems to be approximately six-fold weaker for NBD-daptomycin, suggesting that daptomycin preferentially binds to lipids. This is also proved by the partition coefficient, K_p, which is the ratio of the concentration of bound peptide versus free peptide. Furthermore, the dissociation constant K_d values are comparable determined by both measurements, binding isotherms (Table 2.1) and kinetic measurements (Table 2.2). In addition, a titration experiment with Ca^{2+} as the titrant was conducted showing that the fluorescence intensity reaches a plateau when the concentration of Ca^{2+} is around 41 μM, long before the experimental concentration of calcium (The titration curves are in Appendix A1). Thus calcium can be neglected from the binding equilibrium.

Table 2.1 K_d and K_p of 4 μM daptomycin and NBD-daptomycin binding to different membrane models.

Peptide	K_d (μM) with DMPC/PG	K_d (μM) with POPC/PG	K_p (M) with DMPC/PG	K_p (M) with POPC/PG
Daptomycin	11.0 ± 0.7[a]	15.9	$(1.4 \pm 0.5) \times 10^5$ [a]	9.87×10^4
NBD-daptomycin	62.0	13.7	7.72×10^4	1.56×10^5

[a] This represents the average of two replicates of the binding experiment for daptomycin and DMPC/PG, with a standard deviation of 0.7.

Table 2.2 Kinetic parameters of different peptides binding to DMPC/PG liposomes.

Peptide Concentration	Initial Rate (μM/s)	Rate Constant ($\times 10^{-3}$ $\mu M^{-1} s^{-1}$)	K_d (μM)	Forward Rate Constant from Kintek ($\times 10^{-3}$ $\mu M^{-1} s^{-1}$)
3.36 μM daptomycin	2.8 ± 0.4	3.2 ± 0.5	19 ± 2	0.9 ± 0.1
1.44 μM daptomycin	1.2 ± 0.4	3 ± 1	12 ± 2	1.8 ± 0.8
3.36 μM NBD-daptomycin	2.5 ± 0.4	2.8 ± 0.4	74 ± 6	0.7 ± 0.4
1.44 μM NBD-daptomycin	0.6 ± 0.1	1.5 ± 0.3	85 ± 53	0.32 ± 0.03

2.3.2 Membrane fusion caused by daptomycin

As demonstrated by Jung et al. [70], daptomycin can cause fusion between lipid vesicles when they are composed of a proportion of PG in the presence of calcium. In order to determine whether fusion of vesicles is involved at MIC concentrations, the size of vesicles were measured using PCS, with daptomycin concentrations of 6.3 μM, lipid concentrations of 260 μM, and

calcium concentrations in the range of 0.2 mM to 7 mM, which are similar to the conditions used in Palmer's studies [62, 63, 71]. The measurements were carried out using following lipid compositions: DMPC/DMPG (50%: 50%), POPC (100%), POPC/POPG (50%: 50%), and POPC/POPG/CL (40%: 50%: 10%). As shown in Figure 2.5, fusion occurs rapidly for vesicles composed of DMPC/DMPG. When the experiment is carried out with NBD-daptomycin then higher calcium concentrations are required to trigger the fusion. Moreover, when the experiment is conducted with POPC/POPG, which are with longer unsaturated acyl chains, higher calcium concentrations are required before the occurrence of fusion. Finally, in the case of lipids only containing PC, where no negative headgroup lipids are present, fusion never occurs, which is consistent with the results demonstrated by Jung et al., further suggesting that PG is a necessary component for daptomycin to bind to the membrane. Higher lipid concentrations delay the occur of the fusion which means higher calcium concentrations are required in this case, and the vesicle fusion is independent of whether the experiments are carried out in water or buffer containing 150 mM NaCl.

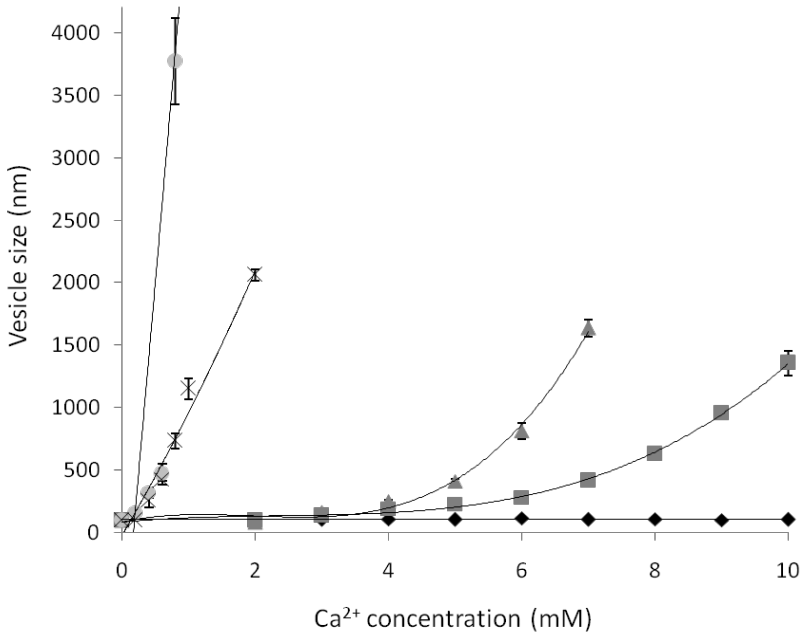

Figure 2.5 Lipid vesicle size as a function of calcium concentration for: DMPC/DMPG (light grey circles), POPC/POPG/CL (grey triangles), POPC/POPG (grey squares), and POPC (black diamonds). The daptomycin concentration was 6.3 µM and the concentration of the lipids was 260 µM. A curve for NBD-daptomycin (6.3 µM) in DMPC/DMPG (260 µM) is also shown using grey X. The data represents the average of four replicates.

Although fusion is not likely to be a significant factor for the mode of action of daptomycin *in vivo*, its presence indeed has an impact for *in vitro* biophysical studies due to the persistent of fusion even after dilution. A serial dilution of the solution containing daptomycin in POPC/POPG/CL and 7 mM Ca^{2+}, when the vesicles are in fused state, is presented in Figure 2.6. Very similar trends were observed for vesicles with the composition of POPC/POPG and DMPC/DMPG.

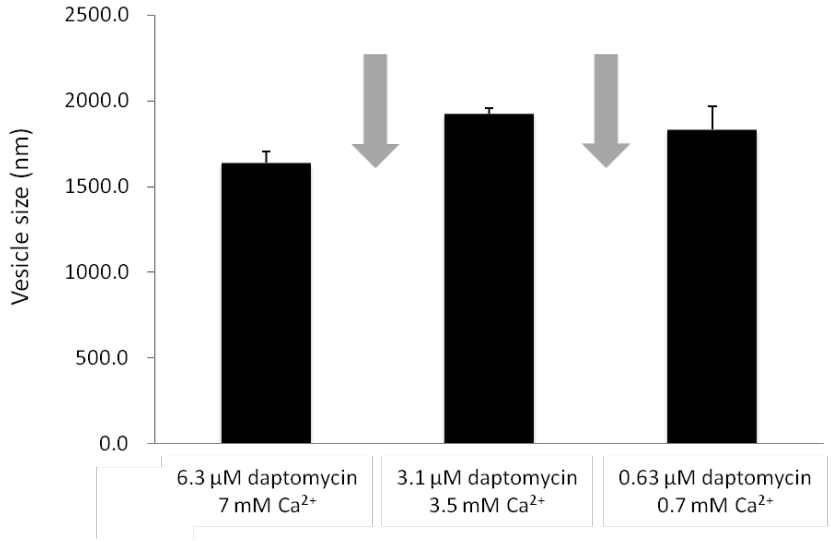

Figure 2.6 Once fusion is established, it is persistent, even after dilution, as seen here for daptomycin in POPC/POPG/CL. The grey arrows indicate first a two fold and then a ten fold dilution relative to the starting concentration (left-most bar). This behavior was also observed for the other lipid compositions tested where fusion was found. The data represents the average of 4 replicates.

2.3.3 Oligomerization at the membrane

Previous experiments performed by Muraih et al. [62] to determine the oligomerization of daptomycin in lipid bilayers, however, were conducted under conditions in which fusion is found to occur. Taking fusion into account, fluorescence experiments performed in [62, 71] were repeated here under conditions where fusion is inhibited to occur. In Figure 2.7, daptomycin in increasing amounts from 0.72 µM to 4.8 µM, with concentration of NBD-labeled daptomycin kept to be 19% of daptomycin, was added to a fixed concentration of 260 µM lipid. When daptomycin oligomers are formed, there is FRET where the NBD can act as an acceptor for the kynurenine residues in the oligomer. The relationship of the amount of FRET observed versus the increasing concentration of daptomycin/NBD-daptomycin is shown in Figure 2.7, with the amount of FRET measured as the emission ratio of NBD to kynurenine. The fluorescence curves

of these measurements can be found in Appendices A2. It is believed that around 96% of the total daptomycin would be bound to lipid vesicles when the daptomycin is at the lowest concentration (0.72 μM). It is shown in fluorescence spectra that both the quenching of kynurenine fluorescence and sensitization of NBD fluorescence increase as the concentration of total daptomycin increases, indicating that daptomycin is able to bind to liposomes without oligomerization. The extent of oligomers formation appears to increase as the concentration of total daptomycin increases, and therefore daptomycin bound to liposomes increases at the same time.

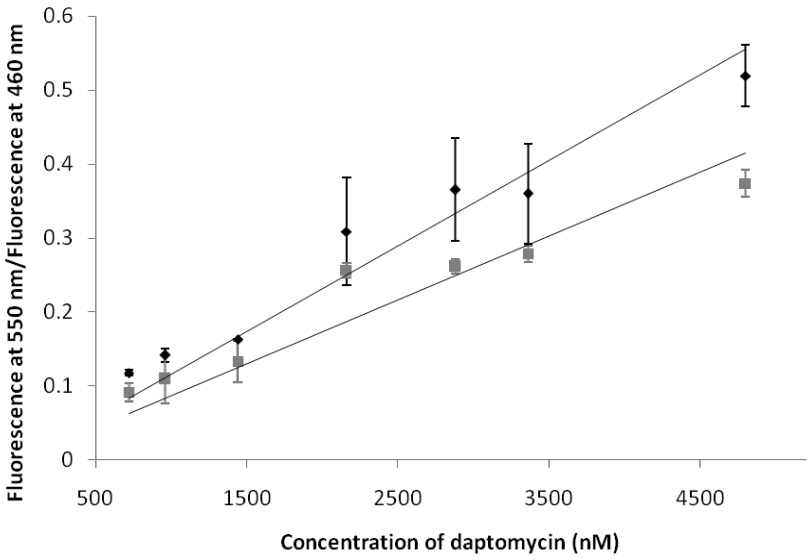

Figure 2.7 Ratio of the fluorescence intensity measured at 546 nm over the intensity measured at 446 nm against the total concentration of daptomycin. Black diamonds represent experiments where the daptomycin and NBD-daptomycin were pre-mixed and the grey squares represent experiments in which the same two components were added sequentially. Two replicates were performed. The error bar represents ± one standard deviation.

When the two-stage addition experiments are repeated, in which case daptomycin was added first and then the NBD-daptomycin, with less FRET expected, both less quenching of native kynurenine fluorescence and sensitization of NBD fluorescence are observed. It is indicated from this result that the oligomers do not re-equilibrate significantly once they are formed over the experimental period, which is around 30 min. However, there is still FRET observed although less, indicating new oligomers are formed consisting of the fraction of free daptomycin and the newly added NBD-daptomycin if the stoichiometry is fixed for the oligomers, or the aggregation increases in size and/or number after the addition of NBD-daptomycin if the stoichiometry is not fixed for the oligomers. The partial oligomerization at lower concentrations was also proved by the observation that with time (from 30 min to 24 h) the signal obtained from a sequential sample converges towards that of the premixed sample, as more NBD-daptomycin in the sequential sample appears in the oligomer (Fluorescence curves can be found in Appendices A3). To conclude, these data suggest a two-stage equilibrium process when daptomycin binds and oligomerizes at the membrane:

$$\mathrm{Dapto} + \mathrm{Lipid} \rightleftharpoons \mathrm{Dapto} \cdot \mathrm{Lipid}$$

$$n\mathrm{Dapto} \cdot \mathrm{Lipid} \rightleftharpoons \mathrm{Dapto}_n \cdot \mathrm{Lipid}$$

In order to further understand the factor that causes increased FRET shown in Figure 2.7, which can be the higher number of donor-acceptor pairs in the case of constant oligomerization subunit number or the larger size of the oligomer in the membrane, another set of experiment was carried out. In this experiment, the concentration of daptomycin was kept constant at either 3.36 μM with Ca^{2+} at 420 μM or 1.44 μM with Ca^{2+} at 180 μM, while the concentration of NBD-daptomycin was different. As performed in a previous study [71], Figure 2.8 shows how the

kynurenine fluorescence changes against donor/acceptor ratio, with the curves consistent to the expectation of the model that demonstrated previously. In Figure 2.8a, the relative kynurenine fluorescence from daptomycin is plotted against the ratio of daptomycin (donor) to NBD-daptomycin (acceptor), which is from about 5:1 to 10:1, with the total concentration of daptomycin and NBD-daptomycin of 1.44 μM and 3.36 μM. Based on the Palmer model [71], this data is further interpreted in terms of the stoichiometry of daptomycin oligomers. The curves in Figure 2.8 represent theoretical oligomerization values calculated using Eq. 2.1. An interesting and intriguing finding obtained from this data performed at two different concentrations, is that the oligomerization number n is concentration-dependent: for 1.44 μM daptomycin the oligomerization number is between 3-4 and for 3.36 μM daptomycin it is around 6-7. This concentration-dependence may, however, rather be an artifact of Palmer's assumption that oligomerization is quantitative. There is an alternative possible explanation that daptomycin at 1.44 μM has a larger proportion of the un-oligomerized daptomycin than that in 3.36 μM, which is consistent with the result shown in Figure 2.7. The experiment is also repeated when daptomycin and NBD-daptomycin are added in a two-stage style, shown Figure 2.8b. In Figure 2.8b, the data for both concentrations 1.44 μM and 3.36 μM are statistically indistinguishable and corresponding to the 1.44 μM data in Figure 2.8a. This data is consistent with the result discussed above that only a slight increase in the formation of oligomers after the addition of NBD-daptomycin over the experimental period.

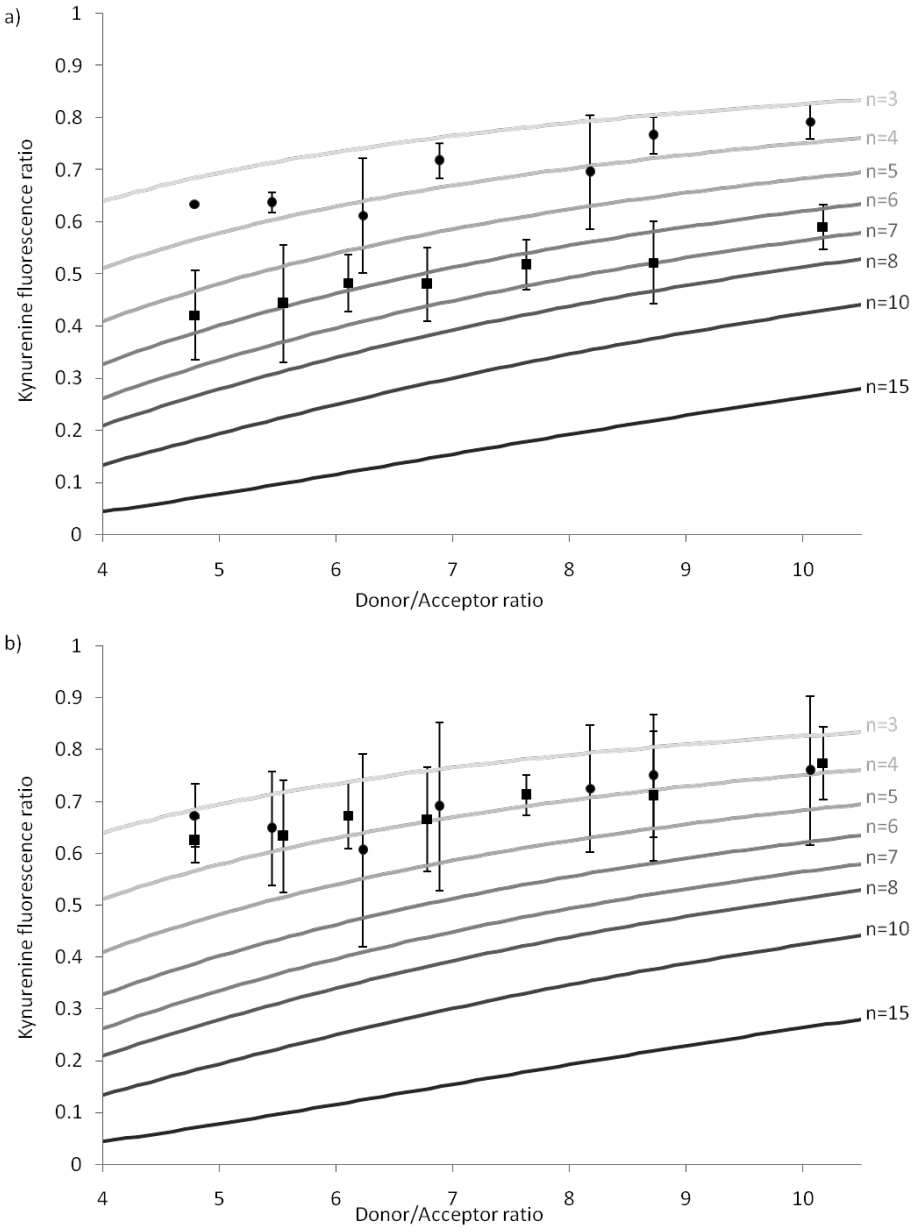

Figure 2.8 Kynurenine fluorescence intensity ratios (with FRET/without FRET) as a function of donor/acceptor ratios for a daptomycin concentration of 3.36 µM (black squares) and 1.44 µM (black circles). The curves represent theoretical values calculated according to Eq. (2) in [71]. a) Pre-mixed samples. b) Sequential addition of donor and acceptor. Four replicates were performed. Measurements were performed after an incubation time of 1 hour.

2.4 Conclusions

In spite of the wide use of daptomycin over the last decade, many details of its mode of action remain to be understood, including the formation of oligomers in the membrane. Palmer and co-workers proposed that daptomycin oligomerizes on lipid and bacterial membranes, with an oligomerization number of 6 to 7 in model membrane systems [62, 71]. A series of fluorescence studies were performed to support this proposal, while the interpretation of the data depended on the following assumptions: 1) all of the daptomycin is bound to the membrane bilayer; 2) daptomycin forms only one type of oligomer in the membrane instantaneously and completely, which means no oligomers with the size smaller than 6-7 formed; 3) the fluorescence measured comes only from oligomers containing daptomycin without any NBD-labeled daptomycin; 4) the oligomer is stable over the time course of experiment and no membrane fusion is caused by the daptomycin. They have not taken the possibility of membrane fusion caused by daptomycin into account, which, however, is present in their work for some of their sample conditions, such as when daptomycin or NBD-daptomycin is at the concentration of about 6 μM in the presence of 5 mM Ca^{2+} in 250-260 μM DMPC/DMPG vesicles, as demonstrated here. They proposed that daptomycin molecules form well-defined pores with a subunit number of 6-7 in a single membrane bilayer, based on the observed FRET. However, when fusion is present, the measured FRET can be due to the daptomycin initially inserted in different liposomes but coming together. In other words, the data, which supports that 6-7 daptomycin molecules are required to perturb the membrane, can also support that 6-7 daptomycin molecules are needed to pull two separate liposomes together leading to the fusion. Both interpretations are possible under many of the sample conditions used by Muraih et al. When concentrations are carefully chosen, the effect of

fusion can be hindered and is no longer a possible explanation of the observed findings. Therefore, fusion has a direct impact on how to interpret the FRET data obtained by Muraih et al. In addition, fusion remains even after dilution, so samples need to be prepared carefully, even if the ultimate concentration at which the experiments are conducted is low. Finally, fusion depends on the lipid type, with the least fusion observed for POPC/PG, indicating that this may be a better membrane model system for investigating the mechanism of daptomycin. Similarly, POPC/PG was considered as a better model the aurein peptide [88].

Although fusion is likely to be an artifact of the *in vitro* biophysical method and probably does not play an important role in the actual mechanism when daptomycin kills bacteria, the proposed model by Palmer and co-workers may need to be modified since the observation of concentration-dependent daptomycin oligomerization. To be specific, the data presented here shows that 1.44 μM daptomycin has a larger fraction of un-oligomerized daptomycin than that of 3.36 μM daptomycin. Considering that the MIC of daptomycin ranges from 20 nM to 5 μM (depending on the different bacteria), this would indicate that the formation of daptomycin oligomers does not occur immediately, at least for certain bacteria, further indicating that daptomycin may first need to accumulate in the membrane in an effort to form large oligomers in the lipid bilayer. It is indeed shown that the time scale of daptomycin killing bacteria is hours based on time-kill curves for 309 nM daptomycin [89], which may be a support to the accumulation requirement discussed here, although applying conclusions drawn from model membranes to complex bacteria should be done with great caution. Once enough daptomycin is accumulated in the membrane, then the membrane is perturbed and/or destroyed either through the formation of an ion channel [56] or through a lipid extracting effect [57], causing leakage of

ions as a result. In summary, the data obtained in this chapter demonstrates that the interpretation of biophysical data associated with daptomycin must be done with caution.

Chapter 3: Characterization of ion permeability in model membranes caused by daptomycin

3.1 Introduction

As mentioned in Chapter 2, once enough daptomycin is accumulated in the membrane, it is proposed that the formation of oligomers leads to membrane perturbation, causing leakage of ions as a result. The nature of the perturbation may be the formation of an ion channel [56], which is an ion-permeable pore in the lipid membrane allowing flow of ions across the membrane. Pore formation is a popular antibacterial mechanism of action for antimicrobial peptides, especially for peptides with amphiphilicity (see more details in section 1.3.3.5). It usually leads to the dissipation of the membrane potential and membrane depolarization. The permeability of those pores can be dependent on the size and charge of ions, displaying ion selectivity.

In a recent study by Zhang et al. [56], the permeability properties of the proposed membrane pores caused by daptomycin were detected by using the liposome model system DMPC/DMPG. A fluorescence assay was used, where a pH-sensitive fluorescence probe pyranine is preloaded in the liposomes. When the liposomes are added into the buffer containing potassium ions or sodium ions at a higher pH, there are two ion concentration gradients across the membrane: the K^+ or Na^+ concentration is higher outside the liposome, while the H^+ concentration is higher inside the liposome. After the pore-forming agent is added to the solution, if there is ion translocation caused by the agent, the pH environment of pyranine is changed, leading to an increase of the fluorescence quantum yield (Figure 3.1). It is concluded from their results that the

pores are selective for cations. They used valinomycin, a potassium-specific ionophore, as a control compared to daptomycin. For valinomycin, peptide in the presence of carbonyl cyanide *m*-chlorophenyl hydrazine (CCCP) induces a large increase of fluorescence intensity, whereas the addition of valinomycin alone has a small effect (Figure 3.2A). The reason of fluorescence increasing higher than 100 A.U. for valinomycin in the presence of CCCP and potassium ions before the addition of Triton-X in Figure 3.2A is not mentioned in the paper. A possible explanation is that the lysis of liposomes after treatment with Triton-X leads to a dilution effect, which decreases the fluorescence intensity. Figure 3.2B shows that for daptomycin the results are slightly different. In this case, ion translocation across the model membrane was only observed when both daptomycin and CCCP were added at the same time, i.e. daptomycin or CCCP alone did not cause any ion flow across the membrane. In previous work to study the selective translocation of ions by the pore-forming aurein peptide, a similar method was used, but CCCP was not required for the translocation of sodium and potassium ions in this case. It is important to note that aurein peptide has been clearly shown to kill *B. subtilis* by pore-formation and selective ion leakage [90].

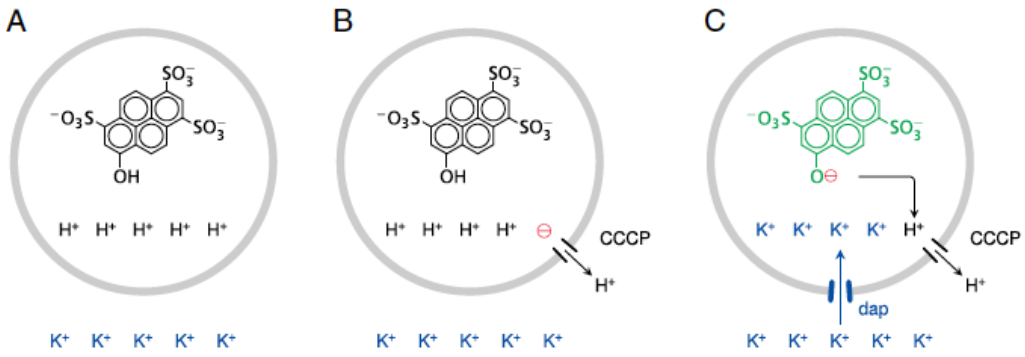

Figure 3.1 Schematic representation of the fluorescence assay using pyranine-loaded liposome to investigate ion permeabilization caused by peptide, using K^+ ions as an example. A) Liposomes preloaded with pyranine were added into the final reaction buffer. B) Addition of proton ionophore allows H^+ ions to translocate through the membrane. C) When peptide such as daptomycin is added and allows K^+ ions to translocate, both ion gradients can dissipate, leading to the increasing pH in the liposome, and the pyranine fluorescence will increase. The figure is adapted from [56].

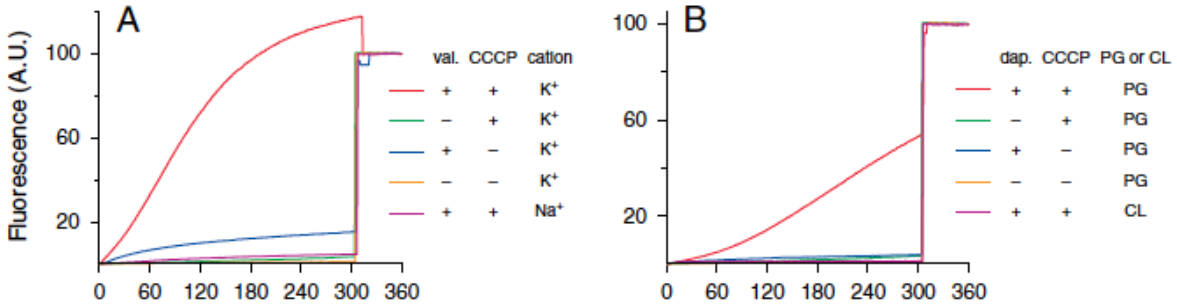

Figure 3.2 Fluorescence traces of pyranine-loaded liposomes after exposure to different permeabilizing agents, added at t=0. The interior pH was 6 and the exterior pH was 8. After 300 s, the vesicles were lysed with Triton-X100. The fluorescence intensity measured after adding Triton was set to 100. A) ion permeabilization caused by valinomycin (0.5 µM) or CCCP (5 nM) or the combination. B) ion permeabilization caused by daptomycin (1 µM) or CCCP (5 nM) or the combination. Figure is adapted from [56].

Zhang et al. explained the reason that CCCP alone causes little change to the pH inside the liposome is due to the restriction of efflux of protons caused by the ensuing diffusion potential [56]. Only when daptomycin is added, which allows the influx of outside ions such as potassium, does an efflux of protons occur, leading to a change of pH inside the liposomes and increasing fluorescence (Figure 3.1). However, other reports have shown that the ionophore CCCP was found to cause rapid membrane depolarization of *S. aureus* at a concentration of 25 μM, similar to the pore-forming antimicrobial agent nisin [53]. Thus, CCCP has been used as a positive control for membrane depolarization studies [91]. Although the concentration of CCCP used by Zhang et al. was much smaller (5 nM), the impact of adding CCCP to DMPC/PG liposomes has never been investigated.

In this chapter, the fluorescence experiments were done to study the ion permeability of POPC/PG and DMPC/PG liposomes caused by daptomycin with or without CCCP to investigate the role of CCCP and how different liposome systems change the permeability. In addition, experiments using the ion-selective pore-forming aurein peptide were done as a comparison.

3.2 Materials and methods

3.2.1 Materials

1-palmitoyl-2-oleoyl-*sn*-glycero-3-phosphocholine (POPC), 1-palmitoyl-2-oleoyl-*sn*-glycero-3-phospho-(1'-*rac*-glycerol) (POPG), 1,2-dimyristoyl-d54-*sn*-glycero-3-phosphocholine (DMPC) and 1,2-dimyristoyl-*sn*-glycero-3-phospho-(1'-rac-glycerol) (DMPG) were purchased from Avanti Polar Lipids, Inc. (Alabaster, AL, USA). Pynanine was purchased from ACROS Organics (NJ, USA). 4-(2-hydroxyethyl)piperazine-1-ethanesulfonic acid (HEPES) and acetonitrile were

purchased from Sigma-Aldrich (St. Louis, MO, USA). Sodium phosphate dibasic, sodium chloride and potassium chloride were purchased from Fisher Scientific (Fair Lawn, NJ, USA). Carbonyl cyanide *m*-chlorophenyl hydrazine (CCCP) was purchased from ACROS Organics (NJ, USA).

3.2.2 *In vitro* ion translocation experiments

The translocation experiments were performed using the method reported in Otis et al.[92], but using an 1:1 POPC/PG or 3:1 DMPC/PG (Avanti Polar Lipids, Alabaster, AL, USA) mixture instead of the phosphatidylcholine (PC) lipid reported in the paper. Briefly, vesicles were prepared by drying POPC and POPG or DMPC and DMPG under vacuum overnight. Lipids were suspended in 2 mL internal buffer containing a pH-sensitive dye (15 mM Na_2HPO_4, 4 mM pyranine, pH 6.2) to reach a concentration of 8.2 mM, and sonicated for 45 min. The suspension was filtered through a 0.22 μM filter. Pyranine not trapped in vesicles was removed by purifying vesicles through a Sephadex G-50 column (1.8 x 15 cm) with external buffer composed of 15 mM Na_2HPO_4 and 200 mM MCl at pH 6.2 as eluent. The MCl solution was either NaCl or KCl.

For the experiments run at room temperature, fluorescence was measured on a Perkin Elmer LS50B luminescence spectrometer. For the experiments run at 15℃ and 35℃, measurements were conducted using Varian Eclipse fluorimeter, equipped with multi-cell holder and temperature control unit. The excitation wavelength is 460 nm and the emission wavelength is 520 nm. For each assay, sensitivity was adjusted to obtain a signal near 900 arbitrary units (a. u.) after the lysis of vesicles by Triton X-100. Stock solutions of daptomycin or aurein 2.3 were prepared in trifluoroethanol (TFE) or water. A series of stock solutions of Ca^{2+} were also

prepared. 100 μL of pyranine loaded vesicle solution was added to 3 mL of external buffer (pH 7.2) in a 1 cm pathlength cuvette equipped with a stir bar. For daptomycin, 14 μL of concentrated Ca^{2+} was also added to reach the corresponding concentration for different concentrations of daptomycin. After stabilization of the signal for 100 s, 20 μL of the peptide solution was added to reach the final concentration specified in results and discussion. For the experiments to investigate the effect of CCCP, CCCP was added after the signal stabilized. Final concentrations of daptomycin, Ca^{2+} and CCCP are specified in the results and discussion session. Fluorescence intensity was measured until the signal reached a plateau, after which 10 μL of a 10% aqueous solution of Triton X-100 was added to completely lyse vesicles for the determination of maximum fluorescence signal. The ion transport efficiency was calculated employing the following formula:

$$\% \text{ transport efficiency} = \frac{F - F_0}{F_{max} - F_0} \quad \text{(Eq. 3.1)}$$

where F_0 is the fluorescence intensity of the liposomes before adding peptide, F is the measured fluorescence intensity, and F_{max} is the fluorescence intensity when the Triton is added.

3.3 Results and discussion

3.3.1 Characterization of ion translocation by aurein peptide

It has been shown that aurein 2.3, an antimicrobial peptide obtained from the frogs can cause selective ion translocation across membranes using 1,2-dipalmitoyl-sn-glycero-3-phospho-(1'-rac-glycerol)/1,2-dihexadecanoyl-sn-glycero-3-phosphoethanolamine (DPPG/DPPE), as well as in the Gram positive bacterium *B. subtilis* [90]. We repeated the same experiment with

POPC/POPG (1:1) liposomes to investigate the ion permeabilization of this model system after treatment with 2.5 μM of aurein 2.3 peptide. The ion translocation efficiency is shown in Figure 3.3. Aurein peptide was dissolved in TFE, so a control experiment in which TFE alone was added was also performed. Figure 3.3 demonstrates that aurein peptide can cause sodium or potassium ions to translocate, with the efficiency of 40% and 80%, respectively. This data is consistent to the previous study suggesting that the aurein peptide oligomers lead to the formation of small toroidal pores in the membrane [90, 93], with preferential leakage of K^+.

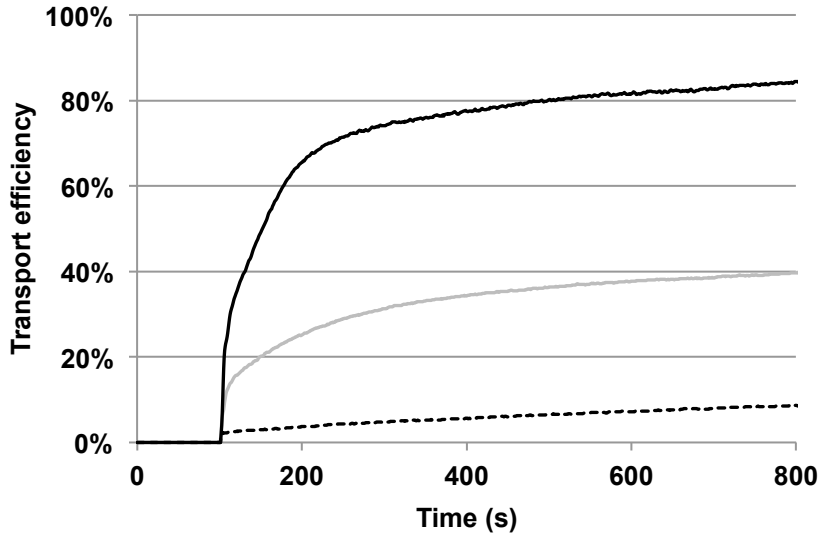

Figure 3.3 Translocation of potassium (black solid curve) and sodium (grey curve) ions into POPC/POPG liposomes. Aurein 2.3 (2.5 μM) was added (peptide/lipid ~1:110) at 100 s. The same volume of TFE only was added for the control run (black dashed curve). Fluorescence intensity after vesicle lysis caused by Triton X-100 was set to 100%. The experiments treated with aurein peptides were repeated three times and the control run were repeated twice. The curves are obtained from the average of data points, with a typical value for the error being ± 1%.

3.3.2 Characterization of ion translocation by daptomycin

In order to investigate if daptomycin can cause ion permeabilization similar to the pore-forming aurein peptide, similar experiments were repeated using daptomycin and Ca^{2+}, required for daptomycin's activity. Experiments were performed with different concentrations of daptomycin and a corresponding concentration of Ca^{2+} where fusion is hindered. The sodium ion transport efficiency (Figure 3.4a) and potassium ion transport efficiency (Figure 3.4b) across POPC/POPG (1:1) vesicles were obtained. The results showed that daptomycin cannot transport sodium and potassium ions across the vesicles, unlike the aurein peptide. Indeed, the curves for vesicles treated with daptomycin are not significantly different from the control. It is suggested from this set of experiment that daptomycin alone is not able to cause ion leakage, a finding which is consistent with the results in Zhang et al. [56].

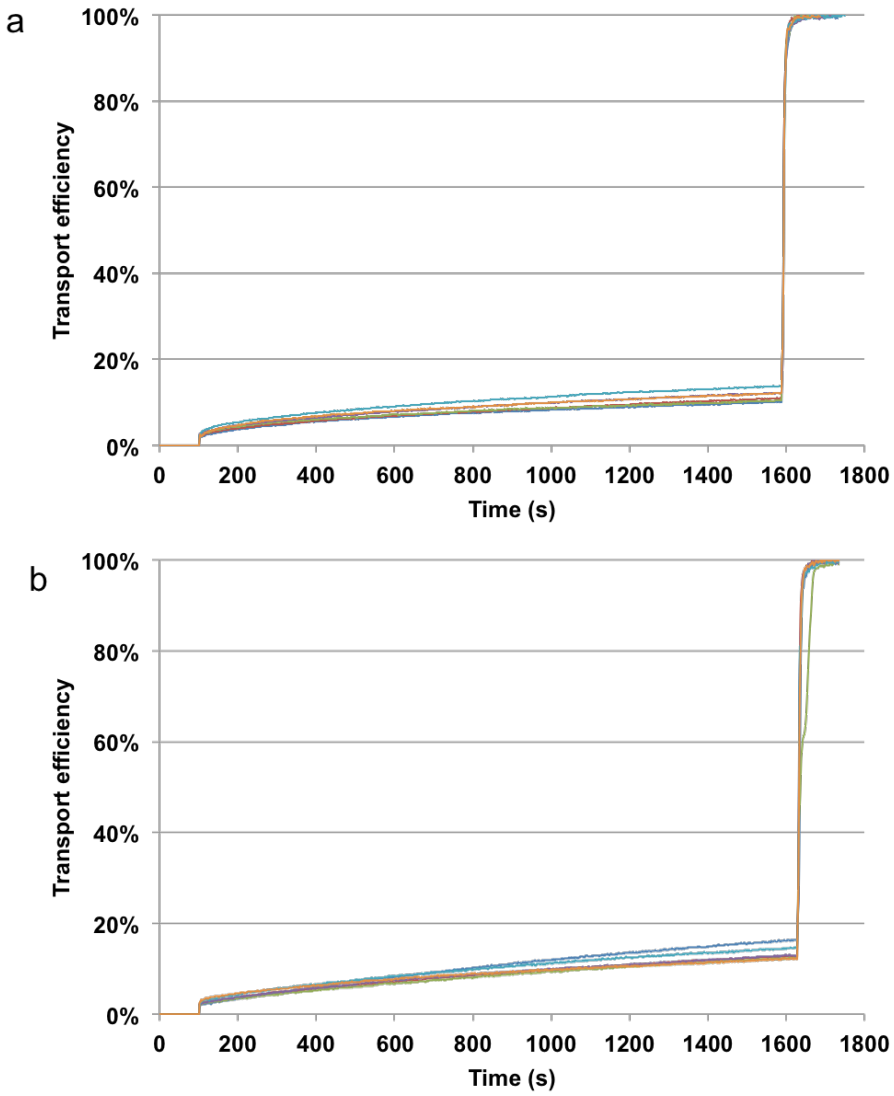

Figure 3.4 Translocation efficiency of sodium (a) and potassium (b) ions into POPC/POPG liposomes. Ca^{2+} was added into the pyranine-loaded vesicles initially. At 100 s, daptomycin at different concentrations was added: 0.72 µM (blue), 1.44 µM (red), 2.16 µM (green), 3.36 µM (purple) and 4.80 µM (cyan). The corresponding concentrations of Ca^{2+} are 90 µM, 180 µM, 270 µM, 420 µM and 600 µM. The control (orange) is TFE alone. Fluorescence intensity after vesicle lysis caused by Triton X-100 was set to 100%. The experiments were repeated twice. The curves are obtained from the average of data points, with a typical value for the error of curves in (a) and (b) being ± 1%.

In Zhang et al.'s study, the authors demonstrated that the addition of ionophore CCCP to daptomycin promoted ion transportation. NMR experiments have been performed showing that there is no interaction between daptomycin and CCCP in buffer with or without the presence of Ca^{2+} (NMR spectra are in Appendix B1). In order to determine whether CCCP can have a similar effect on the ion translocation efficiency under the conditions used here where stable vesicles POPC/POPG are used, the previous experiment was repeated with CCCP. The concentration of daptomycin was kept constant (2.16 μM and 4.80 μM) and the concentration of CCCP was increased. Again an appropriate amount of Ca^{2+} was added to avoid membrane fusion. The little spikes shown Figure 3.5 are due to the addition of CCCP. Surprisingly, there was no obvious increase of the transport efficiency observed after the addition of CCCP, even when the concentration of CCCP was as high as three or four times as the concentration Zhang et al. used.

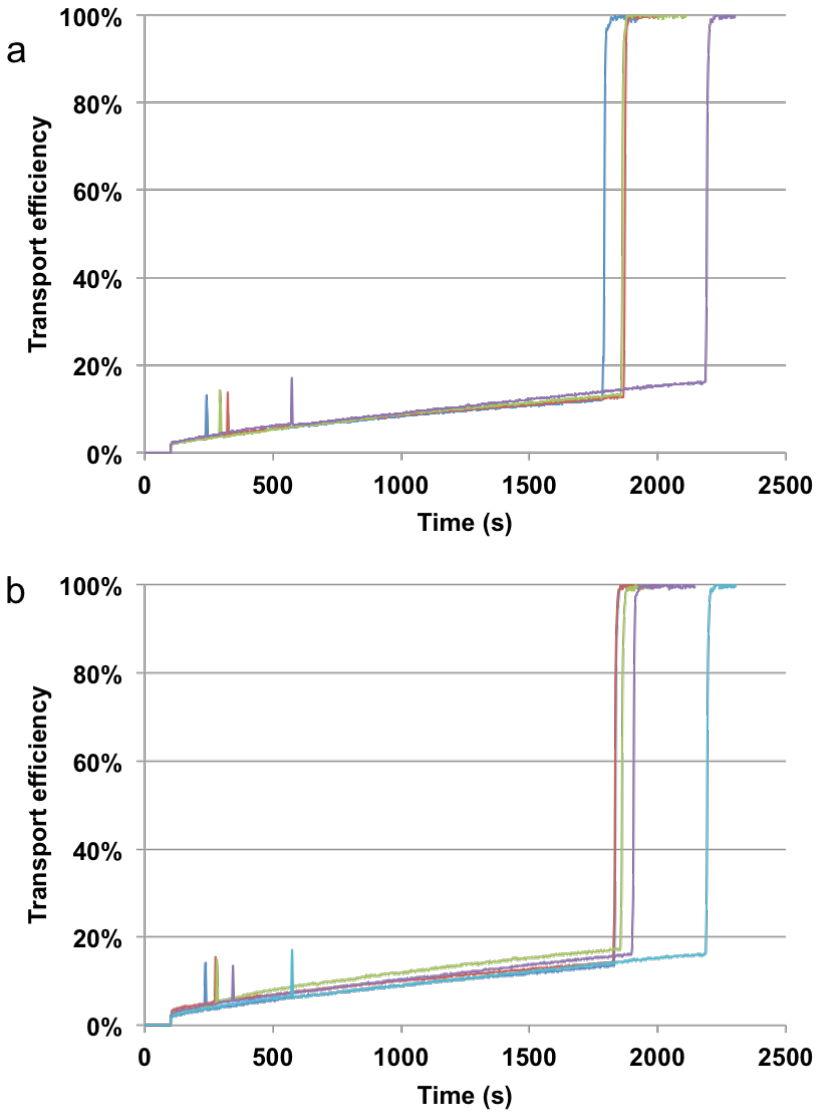

Figure 3.5 Translocation of potassium ions into POPC/POPG liposomes. At 100 s, a) 2.16 µM daptomycin and 270 µM Ca^{2+} or b) 4.80 µM and 600 µM Ca^{2+} was added. Then CCCP at different concentrations was added: a) 10 nM (blue), 20 nM (red), 30 nM (green) and control (purple); b) 20 nM (blue), 40 nM (red), 60 nM (green), 80 nM (purple) and control (cyan). The control is ethanol only, which dissolved CCCP, was added. Fluorescence intensity after vesicle lysis caused by Triton X-100 was set to 100%. This set of experiments has not been repeated.

3.3.3 Stability of vesicles has an effect on the translocation efficiency

The liposomes used by Zhang el al. [56] are consisted of DMPC/PG (3:1). As these lipids undergo a phase transition from the gel to the liquid crystalline phase at 23-24 °C, we have found that DMPC/PG mixtures are often less stable than POPC/PG mixtures (T_m = -2 °C). We therefore repeated the experiments with DMPC/PG (3:1) and CCCP to see whether lipid composition plays a role in daptomycin-induced leakage. DMPC/PG with a 1:1 ratio was tried first. The vesicles were extremely unstable even before adding daptomycin and CCCP, with the rapid increasing of fluorescence intensity (data not shown). This made the experiment to characterize the ion permeability resulting from daptomycin difficult to perform. In addition, DMPC/DMPG with a 3:1 ratio was prepared, which turns out to be unstable as well (Figure 3.6). Although it is not a stable system, it seems that the addition of CCCP does cause an increase of transport efficiency.

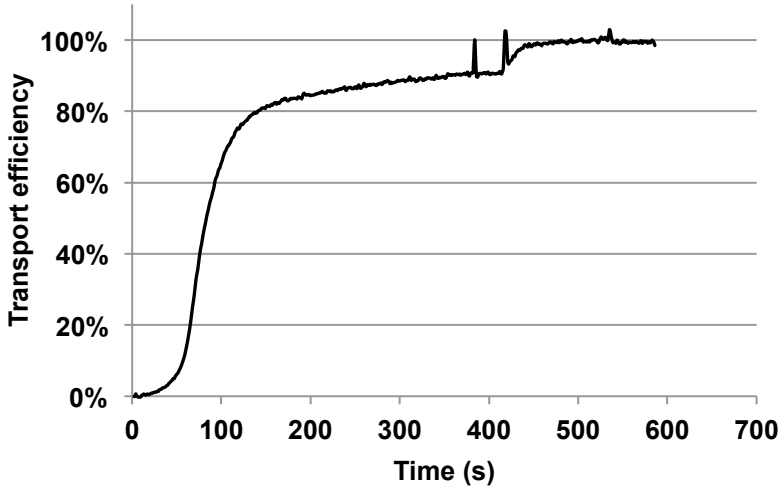

Figure 3.6 Translocation of potassium ions into DMPC/DMPG (3:1) liposomes at room temperature. 270 μM Ca^{2+} was added into the pyranine-loaded vesicles initially. At around 380 s, 2.16 μM of daptomycin was added after the signal reached the plateau. At around 400 s, 10 nM CCCP was added to the solution and an increase was observed. At last, Triton X-100 was added to lyse the vesicle at around 520 s. The fluorescence intensity after vesicle lysis was set to 100 %. There is no repeat for this experiment due to the instability of the vesicles.

As mentioned above, the transition temperatures of DMPC and DMPG are 24 ºC and 23 ºC, respectively. To determine whether the phase of the lipid is important, further experiments were carried out at 35 ºC and 15 ºC to investigate the effects of temperature on the stability of DMPC/DMPG (3:1) vesicles, and the ion permeability when daptomycin and CCCP are added. The transport efficiency results after the treatment of 2.16 μM daptomycin and 10 nM CCCP at these two temperatures are shown in Figure 3.7. 270 μM Ca^{2+} was added into the initial solution containing the pyranine-loaded vesicles. For the result obtained at 35 ºC, the transport efficiency of the vesicles kept increasing initially before the addition of daptomycin, indicating the instability of the vesicles under this condition. When 10 nM CCCP was added at about 530 s, the efficiency increased more quickly, suggesting that CCCP has an effect on the transport efficiency

at 35 ºC. When the experiments were carried out at 15 ºC, where the lipids are in the gel phase, the efficiency does not increase after the addition of daptomycin and CCCP.

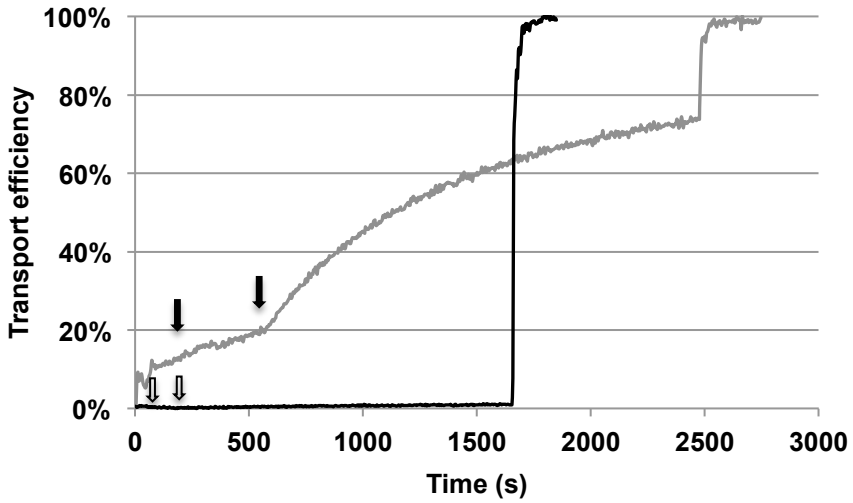

Figure 3.7 Translocation of potassium ions into DMPC/DMPG (3:1) liposomes at 15 ºC (black curve) and 35 ºC (grey curve). 270 µM Ca^{2+} was added into the pyranine-loaded vesicles initially. For the experiment performed at 15 ºC, 2.16 µM daptomycin was added at around 60 s and 10 nM CCCP was added at around 200 s. For the experiment performed at 35 ºC, 2.16 µM daptomycin was added at around 200 s and 10 nM CCCP was added at around 530 s. At last, Triton X-100 was added to lyse the vesicle. The fluorescence intensity after vesicle lysis was set to 100 %.

Since the ionophore CCCP alone can cause rapid membrane leakage at a concentration of 25 µM, similar to the pore-forming antimicrobial agent nisin [53], experiments were conducted to study whether CCCP alone can lead to the increase of ion translocation efficiency observed at 35 ºC or whether the presence of daptomycin is also essential. In this set of experiments, only 2.16 µM of daptomycin was added, or only 10 nM CCCP was added or both of them were added, as shown in Figure 3.8. The control experiment without adding daptomycin or CCCP was also performed. Although under this condition, the vesicles are not very stable, the smallest efficiency was

obtained when vesicles were only treated with daptomycin, which is almost same with the control experiment, while the efficiency was slightly higher for vesicles treated with CCCP, and the highest was obtained upon addition of both daptomycin and CCCP. Similar experiments were done at 15 ºC, but because 10 nM CCCP does not cause any increase in transport (shown in Figure 3.7), a higher concentration of CCCP was used, as shown in Figure 3.9. When only 2.16 μM of daptomycin was added, few ions translocate through the membrane, with the efficiency close to zero. For the vesicles treated with CCCP alone, from 10 nM to 1 μM, the ion translocation efficiency is relatively constant at around 1%. However, when both daptomycin and the higher concentrations of CCCP (0.5 μM and 1 μM) were added, the efficiency increases to 3%-5%, although this number is still quite small compared to results from aurein peptide. Overall, these data show that both daptomycin and CCCP are required to produce some ion permeabilization. The data also show that the permeabilization is small when the lipids are in the gel phase and large when the lipids are in the liquid crystalline phase. In the latter case the amount of leakage is similar to that of aurein (without CCCP) or what was reported by Zhang et al (~40% for potassium transportation) [94].

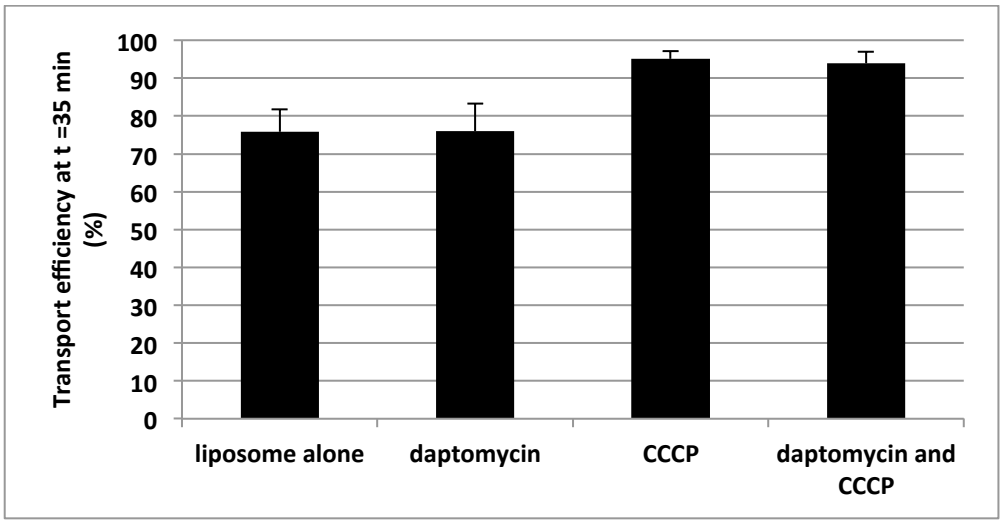

Figure 3.8 Maximum transport efficiency of DMPC/DMPG (3:1) for potassium ions caused by 2.16 µM daptomycin, 10 nM CCCP and a combination of daptomycin and CCCP at 35 ºC. In addition, a control experiment was carried out without adding daptomycin or CCCP. The experiments were repeated twice and the error bar represents one standard deviation.

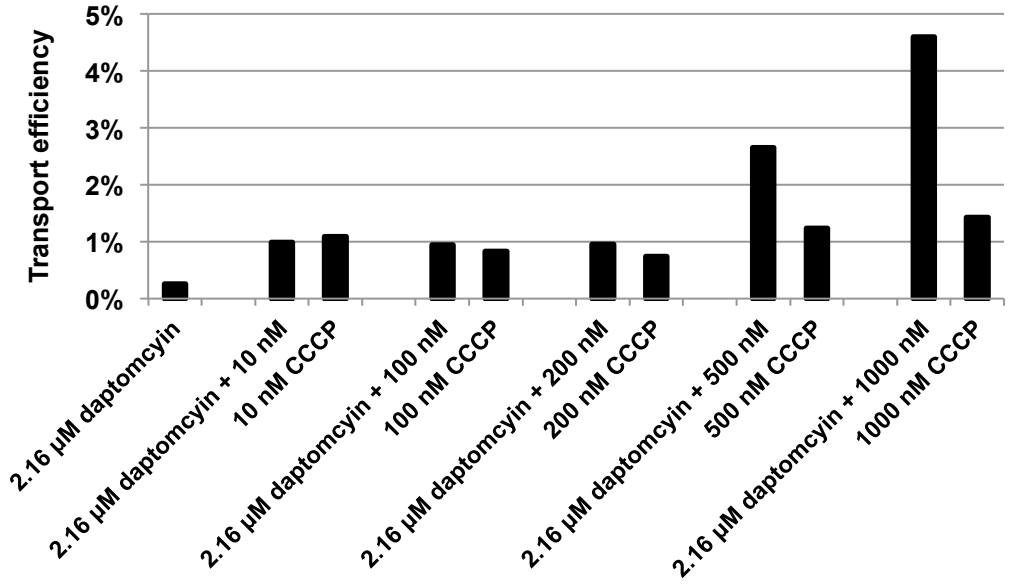

Figure 3.9 Maximum transport efficiency of DMPC/DMPG (3:1) for potassium ions caused by 2.16 µM daptomycin, 10 nM, 100 nM, 200 nM, 500 nM and 1000 nM CCCP and combination of daptomycin and CCCP at 15 ºC. This set of experiments was not repeated.

3.4 Conclusion

The aurein peptide is capable of permeabilizing membranes, allowing the transport of sodium and potassium ions, as shown here by fluorescence experiments using a pH-sensitive fluorescence probe pyranine suggests that aurein peptides form small pores, causing membrane depolarization. Importantly, this effect can be shown without the addition of CCCP. In a previous study, Zhang et al. [56] used a similar method to detect the permeability properties of the membrane caused by daptomycin. In their study, an ionophore CCCP was found to be required in order to observe the translocation of the ions, which is shown in Figure 3.2B. In this chapter, several experiments were carried out to understand how membrane composition and the presence of CCCP affect ion translocation.

When the liposomes are stable, for example POPC/POPG vesicles or DMPC/PG liposomes in gel phase, daptomycin alone or both daptomycin and CCCP does not cause significant ion permeabilization of the membrane. DMPC/PG liposomes were found to be less stable at room temperature, resulting in comparable leakage to the observed by Zhang el al. [56]. Although, Zhang et al. used MES buffer and 250 mM sucrose to stabilize the vesicles, the data presented here suggest that ion leakage may be a consequence of liposome instability. In any case, it is possible to find membrane compositions where daptomycin causes no ion leakage, where under the same conditions the aurein peptides, which function by causing depolarization, are extremely efficient.

Chapter 4: Conclusion and future work

The previous FRET experiments were conducted under conditions where fusion is present, making the interpretation that formation of oligomers in the membrane causes FRET disputable. The condition that fusion is inhibited was determined firstly and FRET experiments were repeated under this condition. The results show that FRET was also observed under the condition where no fusion occurs but the oligomerization subunit number n is concentration-dependent. Thus a two-stage equilibrium process is proposed when the daptomycin binds and oligomerizes in the membrane, in which daptomycin accumulates firstly in the membrane to form larger oligomers, facilitating further effects on the membrane. In addition, a previous study working on the permeability property of daptomycin to get a better understanding of the next step followed by the oligomer formation in the membrane. However, unstable liposomes DMPC/DMPG were used and additional ionophore CCCP was required for ion permeabilization. In Chapter 3, fluorescence experiments were conducted to investigate the ion permeability property of daptomycin on different liposomes, with or without CCCP. For stable liposomes such as POPC/POPG or DMPC/DMPG in gel phase, daptomycin does not cause ion permeabilization of the membrane, suggesting that the membrane depolarization observed for daptomycin is caused by a mechanism that is different from that of the pore-formation aurein peptide. Thus CCCP is not helpful when the liposomes are stable. The work described in this thesis provides evidence leading to a more clear mechanism of daptomycin. Figure 4.1 presents a revised model. Daptomycin firstly inserts into the membrane containing negatively charged lipids. In Figure 4.1B, daptomycin accumulates in the membrane but it does not seem to form a well-defined oligomer. An equilibrium exists between Figure 4.1B and C, so that inserted daptomycin

molecules come together to form a well-defined oligomer in the membrane showing in Figure 4.1C. When the concentration of daptomycin is below or at the MIC, there is no leakage of potassium ions caused by daptomycin.

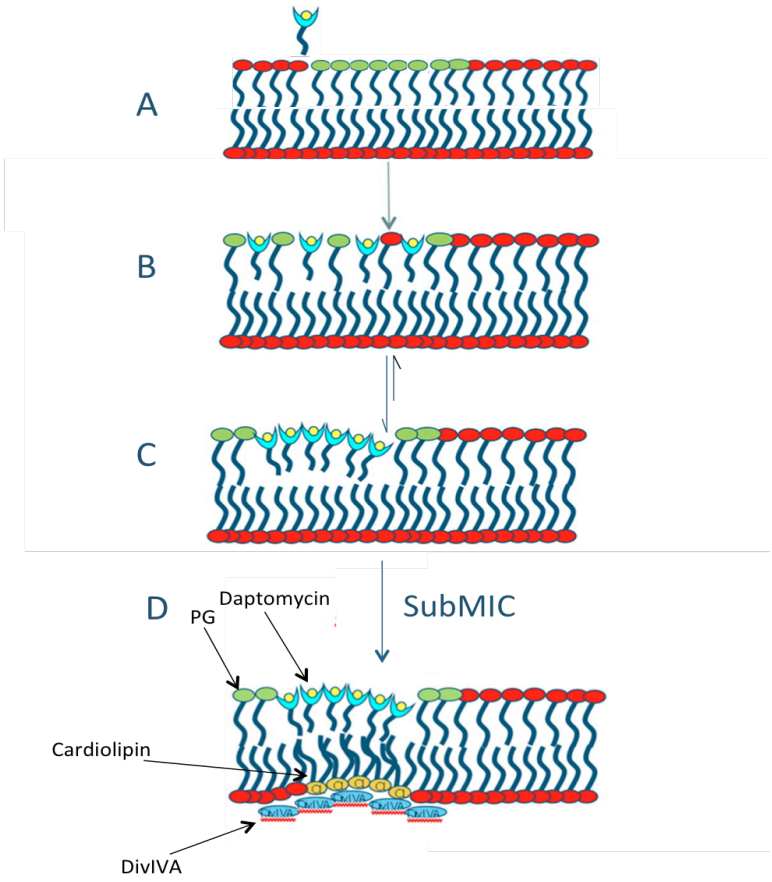

Figure 4.1 A revised model of action of daptomycin. Figure is adapted from [81] with modifications.

Due to the formation of daptomycin oligomers in the membrane, the mode of action of daptomycin shares some similarities with the barrel stave model mentioned in section 1.1.2. However, daptomycin does not cause molecule leakage, which is involved in the barrel stave model. On the other hand, the mode of action of daptomycin may be similar to the aggregate model (refer to section 1.1.2) to some extent as no large pores are formed in the membrane, but

whether daptomycin can inhibit the biosynthesis of crucial cell components is not yet clear. Moreover, the lipid extracting effect caused by daptomycin proposed previously in which model oligomers are composed of both daptomycin and lipids, makes the carpet model (see more in section 1.1.2) a possible mode of action of daptomycin. But in the carpet model, peptides do not insert into the membrane, which is not what was described in Chapter 2. Thus, the mechanism of daptomycin killing bacteria may not be explained by only one single model, but the combination of several models, i.e. barrel stave and aggregate model.

Much remains to be determined about the mechanism of action of daptomycin. In particular, the results described in Chapter 2 do not shed light on whether a daptomycin oligomer interacts with only one or both membrane leaflets. The efficiency of FRET is dependent on the distance between donors and acceptors, which is given by the Förster radius R_0. The R_0 for the unlabeled daptomycin and NBD-daptomycin pair was estimated to be 2.7 nm [62], while the thickness of a lipid bilayer is around 4 nm. Thus in order to answer the question of whether a daptomycin oligomer is situated in one or both leaflets, fluorescent probes that provide a greater effective R_0 are required. Several other fluorescent derivatives that have been tested by Muraih et al. [71] showed a significant reduced antimicrobial activity, indicating that their oligomerization may be affected too. Quantum dots can be considered as a potential donor/acceptor pair to be attached on the daptomycin, the use of which enables the R_0 in the 5-7 nm range. Future FRET experiments can be performed using quantum dots to investigate the subunit number of daptomycin oligomers in the membrane. In addition, the possibilities of other important targets could be investigated, for example the protein DivIVA mentioned in 1.3.3.7, which is recruited at the daptomycin-

induced membrane patches. Further study of the interaction between daptomycin and DivIVA can be performed.

The ion permeability property of daptomycin needs to be investigated in future work, using the vesicles and buffers used in Zhang et al.'s study [56], under conditions where fusion is hindered. The role of CCCP could also be studied in this system. In addition, whether daptomycin at concentrations higher than MIC can cause leakage of potassium ions could be investigated. NMR experiments could be performed to see if CCCP changes the structure of daptomycin in the presence of lipids.

Bibliography

1. Naghavi, M., et al., Global, regional, and national age-sex specific all-cause and cause-specific mortality for 240 causes of death, 1990-2013: a systematic analysis for the Global Burden of Disease Study 2013. *Lancet* **2015,** *385* (9963), 117-171.

2. Spring, M., A brief survey of the history of the antimicrobial agents. *Bulletin of the New York Academy of Medicine* **1975,** *51* (9), 1013-5.

3. Laxminarayan, R., et al., Antibiotic resistance-the need for global solutions. *Lancet Infectious Diseases* **2013,** *13* (12), 1057-1098.

4. Centers for Disease Control and Prevention Antibiotic resistance threats in the United States, 2013. (accessed April 3).

5. Rotem, S.; Mor, A., Antimicrobial peptide mimics for improved therapeutic properties. *Bba-Biomembranes* **2009,** *1788* (8), 1582-1592.

6. Jenssen, H., et al., Peptide antimicrobial agents. *Clin Microbiol Rev* **2006,** *19* (3), 491-+.

7. Nijnik, A.; Hancock, R., Host defence peptides: antimicrobial and immunomodulatory activity and potential applications for tackling antibiotic-resistant infections. *Emerging health threats journal* **2009,** *2*, e1.

8. Fox, J. L., Antimicrobial peptides stage a comeback. *Nat Biotechnol* **2013,** *31* (5), 379-382.

9. Masuda, M., et al., A Novel Anti-Hiv Synthetic Peptide, T-22 ([Tyr5,12,Lys7]-Polyphemusin-Ii). *Biochem Bioph Res Co* **1992,** *189* (2), 845-850.

10. Sumi, C. D., et al., Antimicrobial peptides of the genus Bacillus: a new era for antibiotics. *Can. J. Microbiol.* **2015,** *61* (2), 93-103.

11. Hancock, R. E. W.; Sahl, H. G., Antimicrobial and host-defense peptides as new anti-infective therapeutic strategies. *Nat Biotechnol* **2006,** *24* (12), 1551-1557.

12. Hancock, R. E. W.; Lehrer, R., Cationic peptides: a new source of antibiotics. *Trends Biotechnol* **1998,** *16* (2), 82-88.

13. Sawai, M. V., et al., The NMR structure of human beta-defensin-2 reveals a novel alpha-helical segment. *Biochemistry-Us* **2001,** *40* (13), 3810-3816.

14. Mandard, N., et al., Solution structure of thanatin, a potent bactericidal and fungicidal insect peptide, determined from proton two-dimensional nuclear magnetic resonance data. *Eur J Biochem* **1998,** *256* (2), 404-410.

15. Powers, J. P. S., et al., Structure-activity relationships for the beta-hairpin cationic antimicrobial peptide polyphemusin I. *Bba-Proteins Proteom* **2004,** *1698* (2), 239-250.

16. McManus, A. M., et al., Three-dimensional structure of RK-1: a novel alpha-defensin peptide. *Biochemistry-Us* **2000,** *39* (51), 15757-64.

17. Gesell, J., et al., Two-dimensional H-1 NMR experiments show that the 23-residue magainin antibiotic peptide is an alpha-helix in dodecylphosphocholine micelles, sodium dodecylsulfate micelles, and trifluoroethanol/water solution. *J Biomol Nmr* **1997,** *9* (2), 127-135.

18. Rozek, A., et al., Structure of the bovine antimicrobial peptide indolicidin bound to dodecylphosphocholine and sodium dodecyl sulfate micelles. *Biochemistry-Us* **2000,** *39* (51), 15765-15774.

19. Friedrich, C. L., et al., Structure and mechanism of action of an indolicidin peptide derivative with improved activity against gram-positive bacteria. *J Biol Chem* **2001,** *276* (26), 24015-24022.

20. Giuliani, A., et al., Antimicrobial peptides: an overview of a promising class of therapeutics. *Cent Eur J Biol* **2007,** *2* (1), 1-33.

21. Chen, F. Y., et al., Evidence for membrane thinning effect as the mechanism for peptide-induced pore formation. *Biophys J* **2003,** *84* (6), 3751-3758.

22. Hancock, R. E. W.; Chapple, D. S., Peptide antibiotics. *Antimicrob Agents Ch* **1999,** *43* (6), 1317-1323.

23. Lehrer, R. I.; Ganz, T., Cathelicidins: a family of endogenous antimicrobial peptides. *Curr Opin Hematol* **2002,** *9* (1), 18-22.

24. Matsuzaki, K., et al., An antimicrobial peptide, magainin 2, induced rapid flip-flop of phospholipids coupled with pore formation and peptide translocation. *Biochemistry-Us* **1996,** *35* (35), 11361-11368.

25. Brogden, K. A., Antimicrobial peptides: Pore formers or metabolic inhibitors in bacteria? *Nat Rev Microbiol* **2005,** *3* (3), 238-250.

26. Friedrich, C. L., et al., Antibacterial action of structurally diverse cationic peptides on gram-positive bacteria. *Antimicrob Agents Ch* **2000,** *44* (8), 2086-2092.

27. Dixon, R. A.; Chopra, I., Polymyxin-B and Polymyxin-B Nonapeptide Alter Cytoplasmic Membrane-Permeability in Escherichia-Coli. *J. Antimicrob. Chemother.* **1986,** *18* (5), 557-563.

28. New molecular entities - Cubicin - Daptomycin for injection - CUBIST - First approval in a new class of antibiotics. *Formulary* **2003,** *38* (10), 571-572.

29. Pirri, G., et al., Lipopeptides as anti-infectives: a practical perspective. *Cent Eur J Biol* **2009,** *4* (3), 258-273.

30. de Lucca, A. J.; Walsh, T. J., Antifungal peptides: Novel therapeutic compounds against emerging pathogens. *Antimicrob Agents Ch* **1999,** *43* (1), 1-11.

31. Makovitzki, A., et al., Ultrashort antibacterial and antifungal lipopeptides. *P Natl Acad Sci USA* **2006,** *103* (43), 15997-16002.

32. Balunas, M. J., et al., Dragonamide E, a Modified Linear Lipopeptide from Lyngbya majuscula with Antileishmanial Activity. *J Nat Prod* **2010,** *73* (1), 60-66.

33. Kong, F. M.; Carter, G. T., Structure determination of glycinocins A to D, further evidence for the cyclic structure of the amphomycin antibiotics. *J Antibiot* **2003,** *56* (6), 557-564.

34. Malina, A.; Shai, Y., Conjugation of fatty acids with different lengths modulates the antibacterial and antifungal activity of a cationic biologically inactive peptide. *Biochem J* **2005,** *390*, 695-702.

35. Bunkoczi, G., et al., Structure of the lipopeptide antibiotic tsushimycin. *Acta Crystallogr D* **2005,** *61*, 1160-1164.

36. Avrahami, D.; Shai, Y., Conjugation of a magainin analogue with lipophilic acids controls hydrophobicity, solution assembly, and cell selectivity. *Biochemistry-Us* **2002,** *41* (7), 2254-2263.

37. Epand, R. M., Biophysical studies of lipopeptide-membrane interactions. *Biopolymers* **1997,** *43* (1), 15-24.

38. Sucher, A. J., et al., Echinocandins: The Newest Class of Antifungals. *Ann Pharmacother* **2009,** *43* (10), 1647-1657.

39. Shaligram, N. S.; Singhal, R. S., Surfactin - A Review on Biosynthesis, Fermentation, Purification and Applications. *Food Technol Biotech* **2010,** *48* (2), 119-134.

40. Perron, G. G., et al., Experimental evolution of resistance to an antimicrobial peptide. *P Roy Soc B-Biol Sci* **2006,** *273* (1583), 251-256.

41. Eliopoulos, G. M., et al., Invitro and Invivo Activity of Ly 146032, a New Cyclic Lipopeptide Antibiotic. *Antimicrob. Agents Chemother.* **1986,** *30* (4), 532-535.

42. Kirkpatrick, P., et al., Daptomycin. *Nat. Rev. Drug Discov.* **2003,** *2* (12), 943-4.

43. Fowler, V. G., et al., Daptomycin versus standard therapy for bacteremia and endocarditis caused by Staphylococcus aureus. *N. Engl. J. Med.* **2006,** *355* (7), 653-665.

44. Konafani, Z. A.; Corey, G. R., Daptomycin: a rapidly bactericidal lipopeptide for the treatment of Gram-positive infections. *Expert Rev Anti-Infe* **2007,** *5* (2), 177-184.

45. Debono, M., et al., A21978c, a Complex of New Acidic Peptide Antibiotics - Isolation, Chemistry, and Mass-Spectral Structure Elucidation. *J. Antibiot.* **1987,** *40* (6), 761-777.

46. Boeck, L. D., et al., Deacylation of A21978c, an Acidic Lipopeptide Antibiotic Complex, by Actinoplanes-Utahensis. *J. Antibiot.* **1988,** *41* (8), 1085-1092.

47. Debono, M., et al., Enzymatic and Chemical Modifications of Lipopeptide Antibiotic A21978c - the Synthesis and Evaluation of Daptomycin (Ly146032). *J. Antibiot.* **1988,** *41* (8), 1093-1105.

48. Huber, F. M., et al., The Formation of Daptomycin by Supplying Decanoic Acid to Streptomyces-Roseosporus Cultures Producing the Antibiotic Complex A21978c. *J. Biotechnol.* **1988,** *7* (4), 283-292.

49. Julia, P., et al., Heterologous production of daptomycin in Streptomyces lividans. *J. Ind. Microbiol. Biotechnol.* **2006,** *33* (2), 121-128.

50. Menginlecreulx, D., et al., Inhibition of Peptidoglycan Biosynthesis in Bacillus-Megaterium by Daptomycin. *FEMS Microbiol. Lett.* **1990,** *69* (3), 245-248.

51. Canepari, P., et al., Lipoteichoic Acid as a New Target for Activity of Antibiotics - Mode of Action of Daptomycin (Ly146032). *Antimicrob. Agents Chemother.* **1990,** *34* (6), 1220-1226.

52. Alborn, W. E., et al., Daptomycin Disrupts Membrane-Potential in Growing Staphylococcus-Aureus. *Antimicrob. Agents Chemother.* **1991,** *35* (11), 2282-2287.

53. Silverman, J. A., et al., Correlation of daptomycin bactericidal activity and membrane depolarization in Staphylococcus aureus. *Antimicrob. Agents Chemother.* **2003,** *47* (8), 2538-2544.

54. Laganas, V., et al., In vitro bactericidal activities of daptomycin against Staphylococcus aureus and Enterococcus faecalis are not mediated by inhibition of lipoteichoic acid biosynthesis. *Antimicrob. Agents Chemother.* **2003,** *47* (8), 2682-2684.

55. Cotroneo, N., et al., Daptomycin exerts bactericidal activity without lysis of Staphylococcus aureus. *Antimicrob. Agents Chemother.* **2008,** *52* (6), 2223-2225.

56. Zhang, T. H., et al., Daptomycin forms cation- and size-selective pores in model membranes. *Biochimica Et Biophysica Acta-Biomembranes* **2014,** *1838* (10), 2425-2430.

57. Chen, Y. F., et al., Interaction of Daptomycin with Lipid Bilayers: A Lipid Extracting Effect. *Biochemistry* **2014,** *53* (33), 5384-5392.

58. Allen, N. E., et al., Inhibition of Peptidoglycan Biosynthesis in Gram-Positive Bacteria by Ly146032. *Antimicrob. Agents Chemother.* **1987,** *31* (7), 1093-1099.

59. Boaretti, M.; Canepari, P., Identification of Daptomycin-Binding Proteins in the Membrane of Enterococcus-Hirae. *Antimicrob. Agents Chemother.* **1995,** *39* (9), 2068-2072.

60. Allen, N. E., et al., Inhibition of Membrane Potential-Dependent Amino-Acid-Transport by Daptomycin. *Antimicrob. Agents Chemother.* **1991,** *35* (12), 2639-2642.

61. Steenbergen, J. N., et al., Daptomycin: a lipopeptide antibiotic for the treatment of serious Gram-positive infections. *J. Antimicrob. Chemother.* **2005,** *55* (3), 283-288.

62. Muraih, J. K., et al., Oligomerization of daptomycin on membranes. *Biochimica Et Biophysica Acta-Biomembranes* **2011,** *1808* (4), 1154-1160.

63. Muraih, J. K., et al., Characterization of daptomycin oligomerization with perylene excimer fluorescence: Stoichiometric binding of phosphatidylglycerol triggers oligomer formation. *Biochimica Et Biophysica Acta-Biomembranes* **2012,** *1818* (3), 673-678.

64. Tempelaars, M. H., et al., Comparative Analysis of Antimicrobial Activities of Valinomycin and Cereulide, the Bacillus cereus Emetic Toxin. *Appl. Environ. Microbiol.* **2011,** *77* (8), 2755-2762.

65. Jung, D., et al., Structural transitions as determinants of the action of the calcium-dependent antibiotic daptomycin. *Chem. Biol.* **2004,** *11* (7), 949-957.

66. Ho, S. W., et al., Effect of divalent cations on the structure of the antibiotic daptomycin. *European Biophysics Journal with Biophysics Letters* **2008,** *37* (4), 421-433.

67. Scott, W. R. P., et al., NMR structural studies of the antibiotic lipopeptide daptomycin in DHPC micelles. *Biochimica Et Biophysica Acta-Biomembranes* **2007,** *1768* (12), 3116-3126.

68. Ball, L. J., et al., NMR structure determination and calcium binding effects of lipopeptide antibiotic daptomycin. *Organic & biomolecular chemistry* **2004,** *2* (13), 1872-8.

69. Rotondi, K. S.; Gierasch, L. M., A well-defined amphipathic conformation for the calcium-free cyclic lipopeptide antibiotic, daptomycin, in aqueous solution. *Biopolymers* **2005,** *80* (2-3), 374-385.

70. Jung, D., et al., Lipid-specific binding of the calcium-dependent antibiotic daptomycin leads to changes in lipid polymorphism of model membranes. *Chem. Phys. Lipids* **2008,** *154* (2), 120-128.

71. Muraih, J. K.; Palmer, M., Estimation of the subunit stoichiometry of the membrane-associated daptomycin oligomer by FRET. *Biochimica Et Biophysica Acta-Biomembranes* **2012,** *1818* (7), 1642-1647.

72. Zhang, T. H., et al., Mutual inhibition through hybrid oligomer formation of daptomycin and the semisynthetic lipopeptide antibiotic CB-182,462. *Biochimica Et Biophysica Acta-Biomembranes* **2013,** *1828* (2), 302-308.

73. Hobbs, J. K., et al., Consequences of daptomycin-mediated membrane damage in Staphylococcus aureus. *J. Antimicrob. Chemother.* **2008,** *62* (5), 1003-1008.

74. Xing, Y. H., et al., Daptomycin exerts rapid bactericidal activity against Bacillus anthracis without disrupting membrane integrity. *Acta Pharmacol. Sin.* **2014,** *35* (2), 211-218.

75. Tieleman, D. P.; Marrink, S. J., Lipids out of equilibrium: Energetics of desorption and pore mediated flip-flop. *JACS* **2006,** *128* (38), 12462-12467.

76. Bayer, A. S., et al., Mechanisms of daptomycin resistance in Staphylococcus aureus: role of the cell membrane and cell wall. *Antimicrobial Therapeutics Reviews: The Bacterial Cell Wall as an Antimicrobial Target* **2013,** *1277*, 139-158.

77. Cui, L. Z., et al., Correlation between reduced daptomycin susceptibility and vancomycin resistance in vancomycin-intermediate Staphylococcus aureus. *Antimicrob. Agents Chemother.* **2006,** *50* (3), 1079-1082.

78. Friedman, L., et al., Genetic changes that correlate with reduced susceptibility to daptomycin in Staphylococcus aureus. *Antimicrob. Agents Chemother.* **2006,** *50* (6), 2137-2145.

79. Arias, C. A., et al., Genetic Basis for In Vivo Daptomycin Resistance in Enterococci. *N. Engl. J. Med.* **2011,** *365* (10), 892-900.

80. Davlieva, M., et al., Biochemical Characterization of Cardiolipin Synthase Mutations Associated with Daptomycin Resistance in Enterococci. *Antimicrob. Agents Chemother.* **2013,** *57* (1), 289-296.

81. Pogliano, J., et al., Daptomycin-Mediated Reorganization of Membrane Architecture Causes Mislocalization of Essential Cell Division Proteins. *J. Bacteriol.* **2012,** *194* (17), 4494-4504.

82. Wale, L. J., et al., Scanning Electronmicroscopy of Staphylococcus Aureus and Enterococcus Faecalis Exposed to Daptomycin. *J. Med. Microbiol.* **1989,** *30* (1), 45-49.

83. Marsden, H. R., et al., Model systems for membrane fusion. *Chem. Soc. Rev.* **2011,** *40* (3), 1572-1585.

84. Ruzza, P., et al., Cell-Penetrating Peptides: A Comparative Study on Lipid Affinity and Cargo Delivery Properties. *Pharmaceuticals* **2010,** *3* (4), 1045-1062.

85. Drin, G., et al., Physico-chemical requirements for cellular uptake of pAntp peptide - Role of lipid-binding affinity. *Eur. J. Biochem.* **2001,** *268* (5), 1304-1314.

86. Schwarz, G., et al., Thermodynamic Analysis of Incorporation and Aggregation in a Membrane - Application to the Pore-Forming Peptide Alamethicin. *Biochim. Biophys. Acta* **1986,** *861* (1), 141-151.

87. Hawrani, A., et al., Thermodynamics of RTA3 peptide binding to membranes and consequences for antimicrobial activity. *Biochimica Et Biophysica Acta-Biomembranes* **2010,** *1798* (6), 1254-1262.

88. Cheng, J. T. J., et al., The importance of bacterial membrane composition in the structure and function of aurein 2.2 and selected variants. *Biochimica Et Biophysica Acta-Biomembranes* **2011,** *1808* (3), 622-633.

89. Dugourd, D., et al., Antimicrobial Properties of MX-2401, an Expanded-Spectrum Lipopeptide Active in the Presence of Lung Surfactant. *Antimicrob. Agents Chemother.* **2011,** *55* (8), 3720-3728.

90. Wenzel, M., et al., Antimicrobial Peptides from the Aurein Family Form Ion-Selective Pores in Bacillus subtilis. *ChemBioChem* **2015**.

91. Mensa, B., et al., Comparative Mechanistic Studies of Brilacidin, Daptomycin, and the Antimicrobial Peptide LL16. *Antimicrob. Agents Chemother.* **2014,** *58* (9), 5136-5145.

92. Otis, F., et al., How Far Can a Sodium Ion Travel within a Lipid Bilayer? *JACS* **2011,** *133* (17), 6481-6483.

93. Cheng, J. T. J., et al., Effect of Membrane Composition on Antimicrobial Peptides Aurein 2.2 and 2.3 From Australian Southern Bell Frogs. *Biophys. J.* **2009,** *96* (2), 552-565.

94. Zhang, T. H., et al., Cardiolipin Prevents Membrane Translocation and Permeabilization by Daptomycin. *J. Biol. Chem.* **2014,** *289* (17), 11584-11591.

Appendices

Appendix A

A.1 Titration curves of titrating daptomycin in POPC/PG liposomes with Ca^{2+} solution

Titration curves of titrating 4 μM daptomycin in 260 μM POPC/PG liposomes with increasing concentrations (indicated in the figure below) of Ca^{2+} solution.

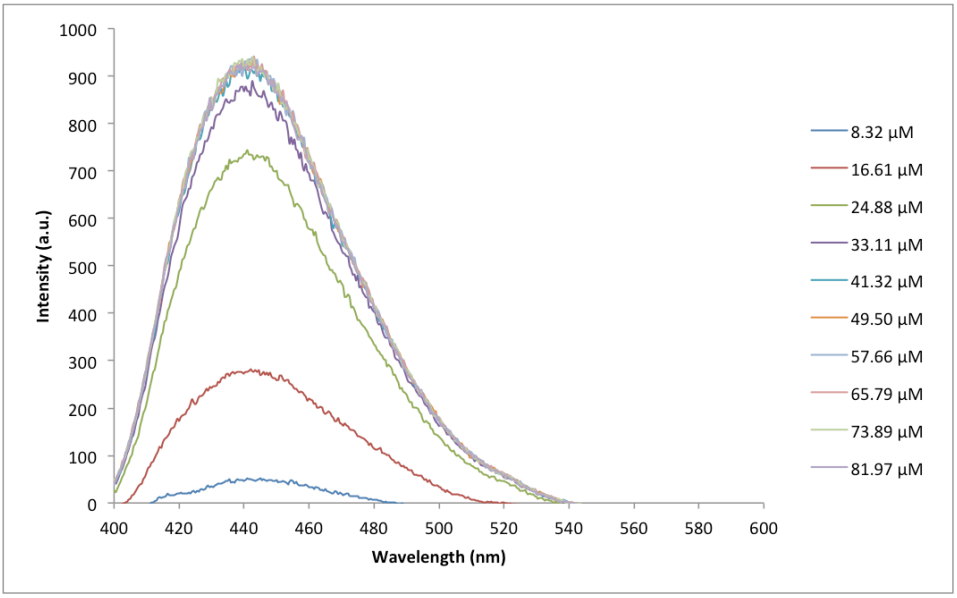

A.2 Fluorescence curves obtained from daptomycin with increasing concentrations

Fluorescence curves obtained from daptomycin with increasing concentrations, keeping relative ratio of daptomycin to NBD-daptomycin and daptomycin to calcium constant. (a) 720 nM of daptomycin, 136.5 nM of NBD-daptomycin and 90 μM of Ca^{2+}; (b) 960 nM of daptomycin, 182 nM of NBD-daptomycin and 120 μM of Ca^{2+}; (c) 1440 nM of daptomycin, 273 nM of NBD-daptomycin and 180 μM of Ca^{2+}; (d) 2160 nM of daptomycin, 409.5 nM of NBD-daptomycin and 270 μM of Ca^{2+}; (e) 2880 nM of daptomycin, 546 nM of NBD-daptomycin and 360 μM of Ca^{2+}; (f) 3360 nM of daptomycin, 637 nM of NBD-daptomycin and 420 μM of Ca^{2+}; (g) 4800 nM of daptomycin, 910 nM of NBD-daptomycin and 600 μM of Ca^{2+}.

a

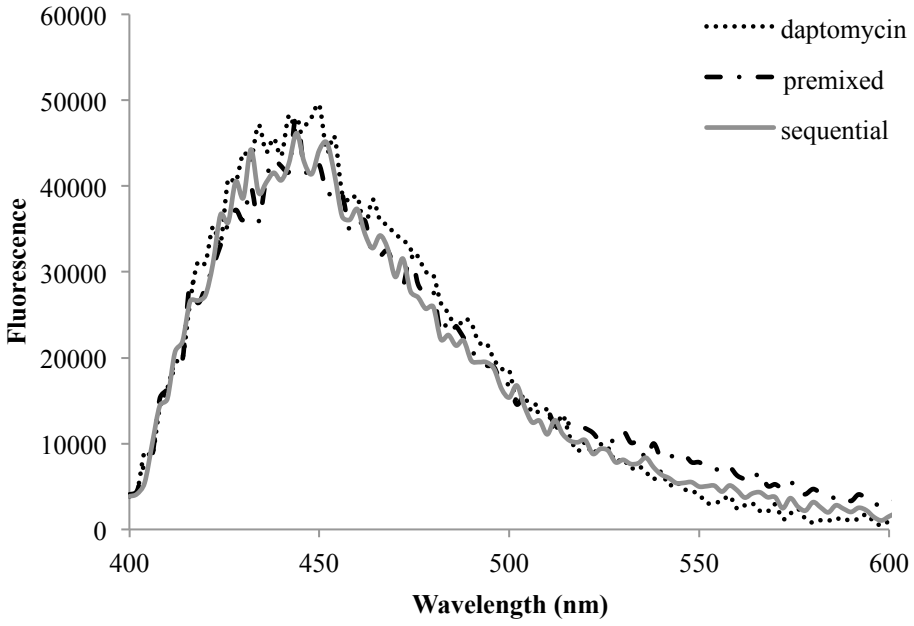

b

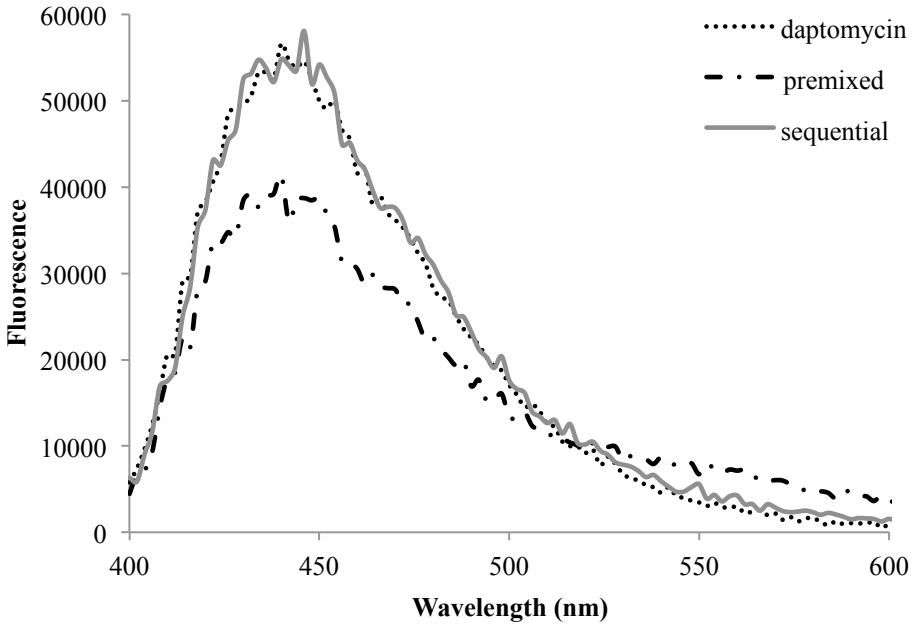
60000
50000
40000
30000
20000
10000
0
Fluorescence
400
450
500
550
600
Wavelength (nm)
daptomycin
premixed
sequential

c

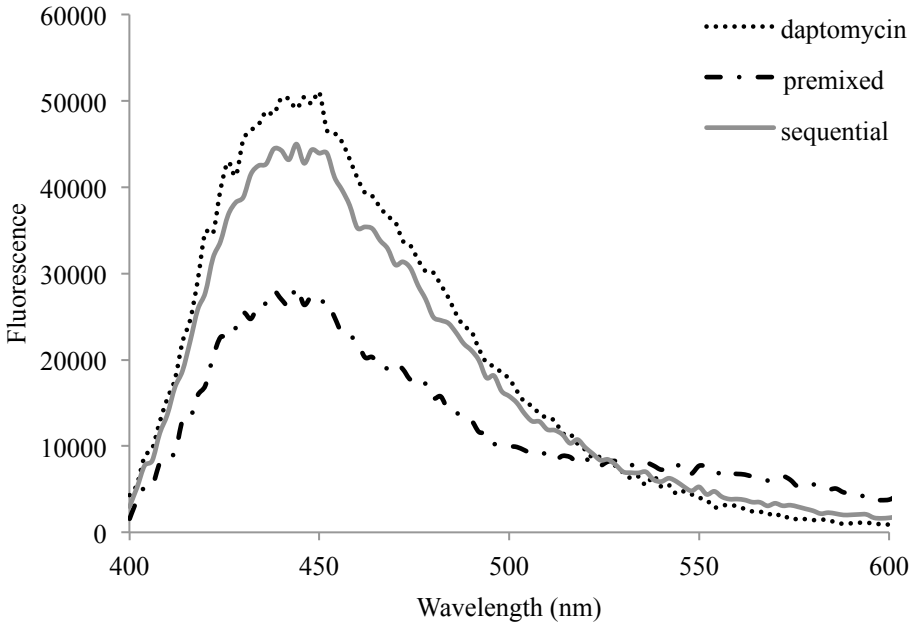
60000
50000
40000
30000
20000
10000
0
Fluorescence
400
450
500
550
600
Wavelength (nm)
daptomycin
premixed
sequential

d

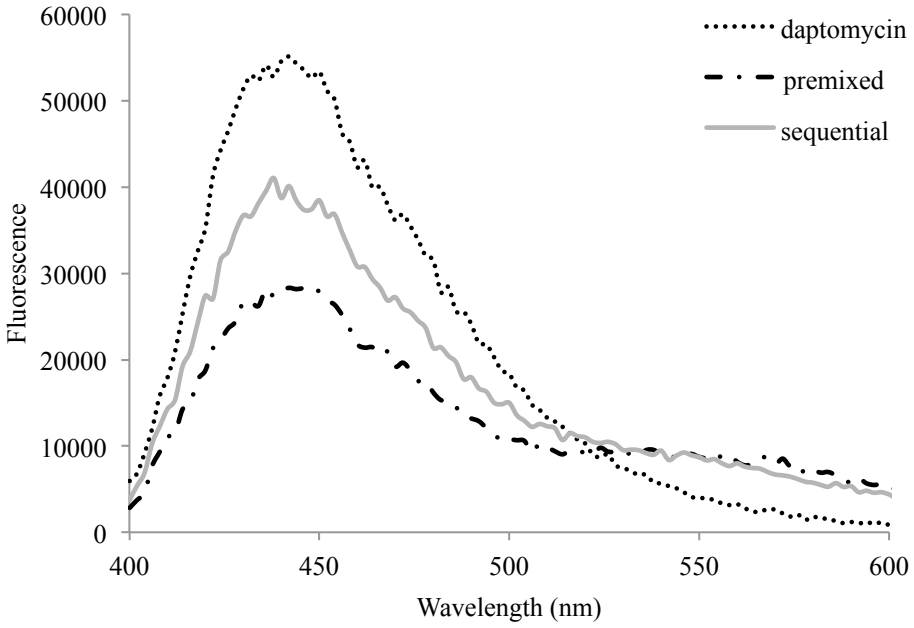
60000
50000
40000
30000
20000
10000
0
Fluorescence
400
450
500
550
600
Wavelength (nm)
daptomycin
premixed
sequential

e

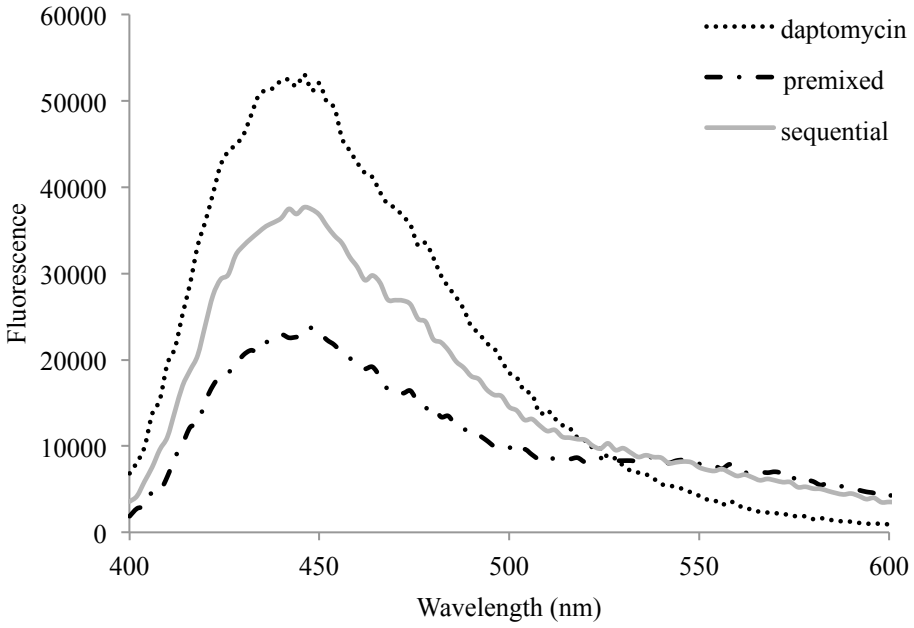
60000
50000
40000
30000
20000
10000
0
Fluorescence
400
450
500
550
600
Wavelength (nm)
daptomycin
premixed
sequential

f

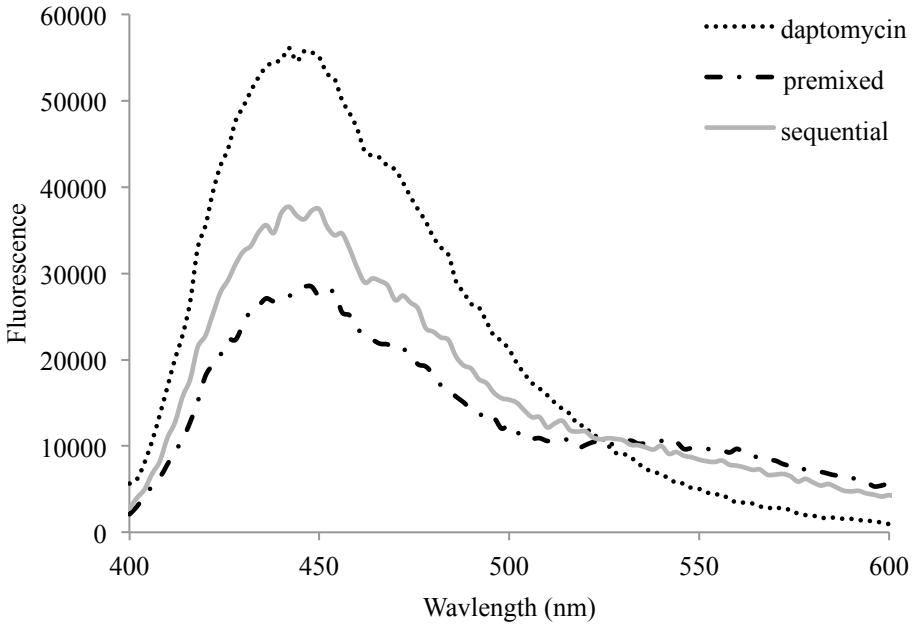
60000
50000
40000
30000
20000
10000
0
Fluorescence
400
450
500
550
600
Wavlength (nm)
daptomycin
premixed
sequential

g

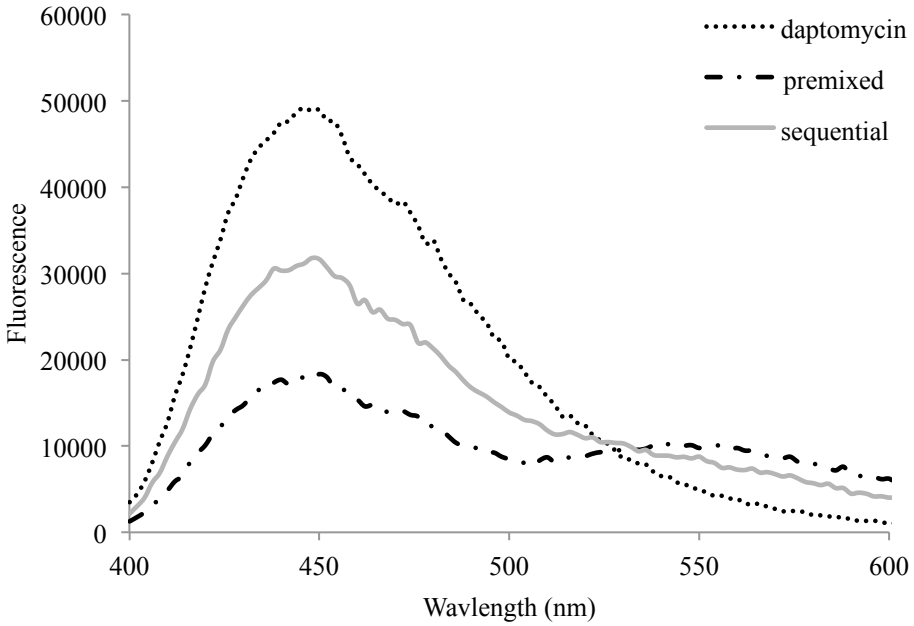
60000
50000
40000
30000
20000
10000
0
Fluorescence
400
450
500
550
600
Wavlength (nm)
daptomycin
premixed
sequential

A.3 Fluorescence curves of daptomycin and NBD-daptomycin added as pre-mixed sample and sequential sample into liposomes with time

Fluorescence curves of 2880 nM of daptomycin, 546 nM of NBD-daptomycin and 360 μM of Ca^{2+} added into liposomes in two styles, pre-mixed or added sequentially. (a) Measurements taken after 30 min; (b) Measurements taken after 1 h; (c) Measurements taken after 18 h; (d) Measurements taken after 24 h.

a

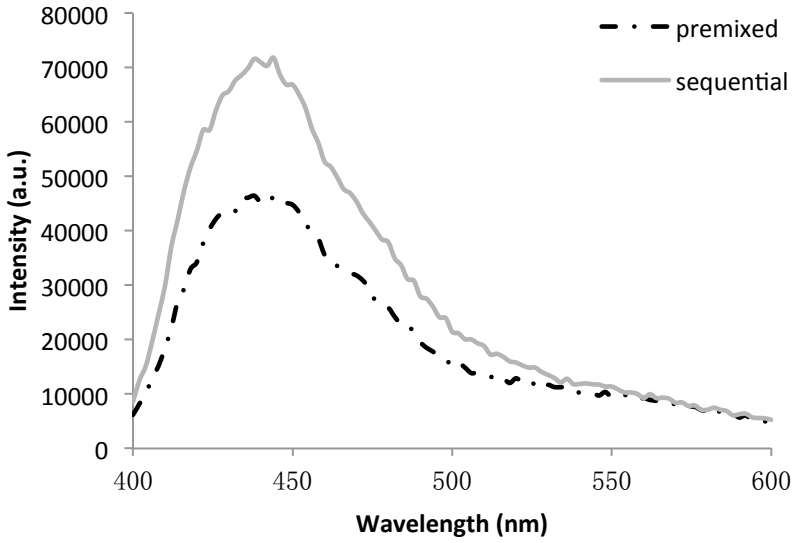

b

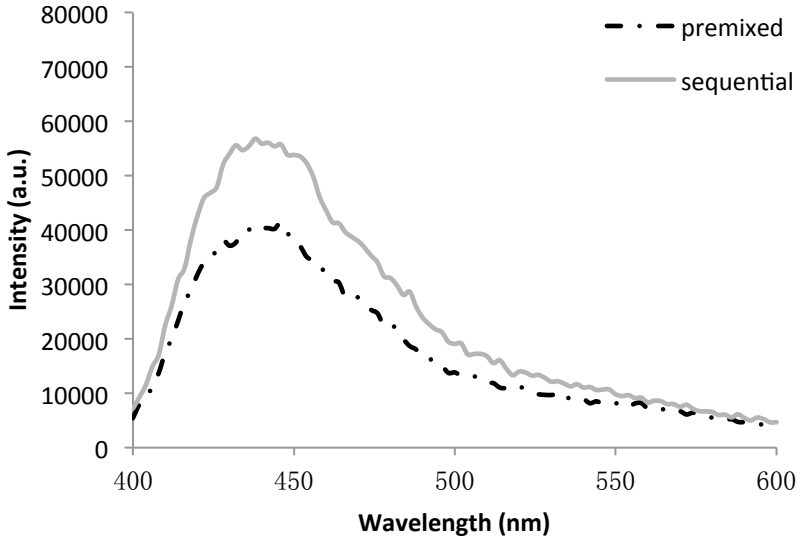
premixed
sequential
Intensity (a.u.)
80000
70000
60000
50000
40000
30000
20000
10000
0
400
450
500
550
600
Wavelength (nm)

c

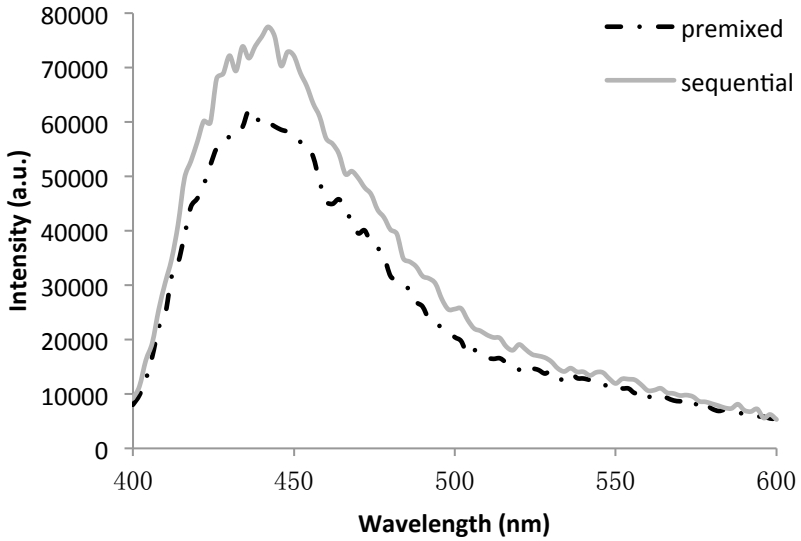
premixed
sequential
Intensity (a.u.)
80000
70000
60000
50000
40000
30000
20000
10000
0
400
450
500
550
600
Wavelength (nm)

d

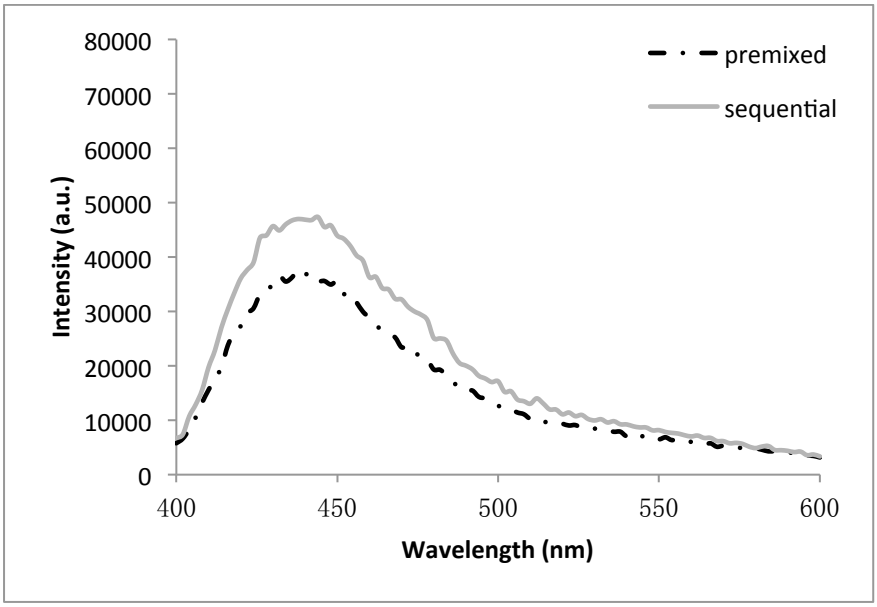
80000
70000
60000
50000
40000
30000
20000
10000
0
Intensity (a.u.)
400
450
500
550
600
Wavelength (nm)
premixed
sequential

Appendix B

B.1 1D ^{1}H NMR spectra of daptomycin and CCCP with increasing concentrations, with/without Ca^{2+} in phosphate buffer

1D ^{1}H NMR spectra of daptomycin and CCCP with increasing concentrations, with/without Ca^{2+} in phosphate buffer with the pH of 6.2. (a) 0.19 mM of daptomycin in 15 mM phosphate buffer; (b) 0.19 mM of daptomycin and 0.97 μM of CCCP in 15 mM phosphate buffer; (c) 0.19 mM of daptomycin and 1.93 μM of CCCP in 15 mM phosphate buffer; (d) 0.19 mM of daptomycin and 4.83 μM of CCCP in 15 mM phosphate buffer; (e) 0.2 mM of daptomycin and 0.5 mM of Ca^{2+} in 7.5 mM phosphate buffer; (f) 0.2 mM of daptomycin, 0.97 μM of CCCP and 0.5 mM of Ca^{2+} in 7.5 mM phosphate buffer; (g) 0.2 mM of daptomycin, 1.93 μM of CCCP and 0.5 mM of Ca^{2+} in 7.5 mM phosphate buffer; (h) 0.2 mM of daptomycin, 4.83 μM of CCCP and 0.5 mM of Ca^{2+} in 7.5 mM phosphate buffer.

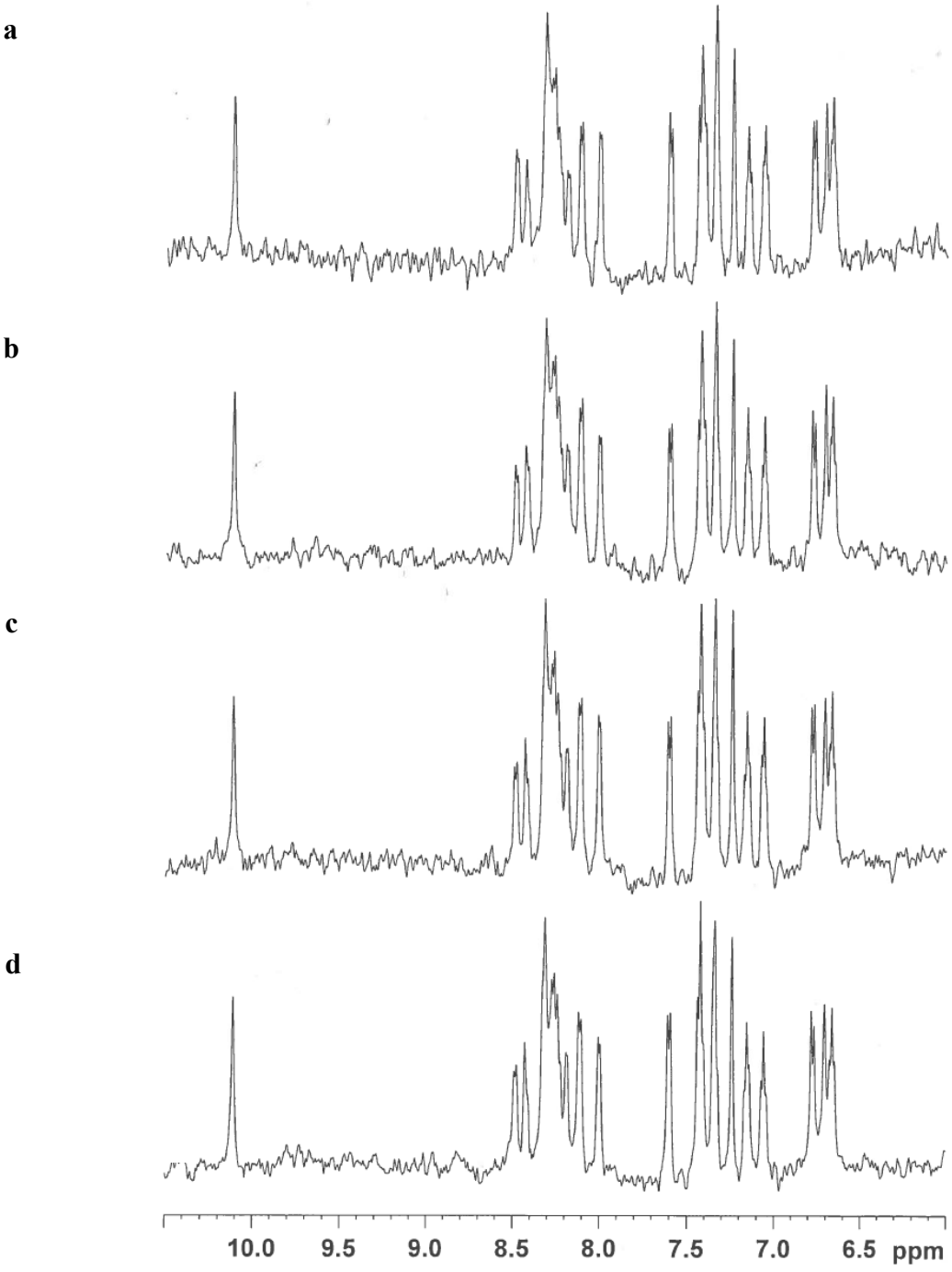
a
b
c
d
10.0
9.5
9.0
8.5
8.0
7.5
7.0
6.5
ppm

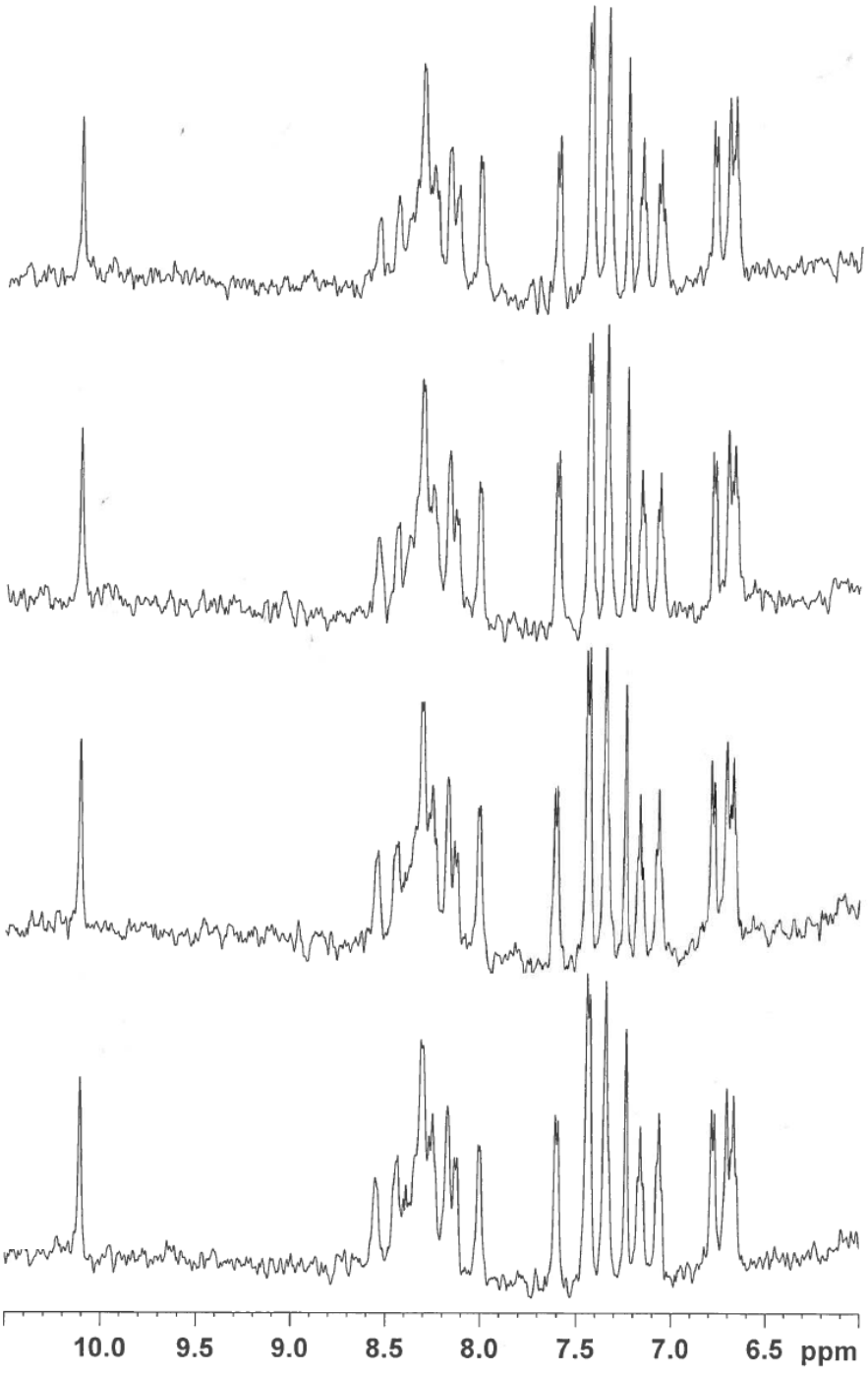
e
f
g
h
10.0
9.5
9.0
8.5
8.0
7.5
7.0
6.5
ppm